# ResearchOnline@JCU



This is the author-created version of the following work:

Kamel, Michael S.A., Al-Jumaili, Ahmed, Oelgemoeller, Michael, and Jacob, Mohan V. (2022) *Inorganic nanoparticles to overcome efficiency inhibitors of organic photovoltaics: An in-depth review.* Renewable and Sustainable Energy Reviews, 166.

Access to this file is available from:

https://researchonline.jcu.edu.au/74836/

© 2022 Published by Elsevier Ltd.

Please refer to the original source for the final version of this work:

https://doi.org/10.1016/j.rser.2022.112661

# Inorganic nanoparticles to overcome efficiency inhibitors of organic photovoltaics: an in-depth review

Michael S. A. Kamelab, Ahmed Al-jumailiac, Michael Oelgemöllerd, Mohan V. Jacob \*a

<sup>a</sup> Electronic Materials Research Lab, College of Science and Engineering, James Cook University,

Townsville 4811, Australia

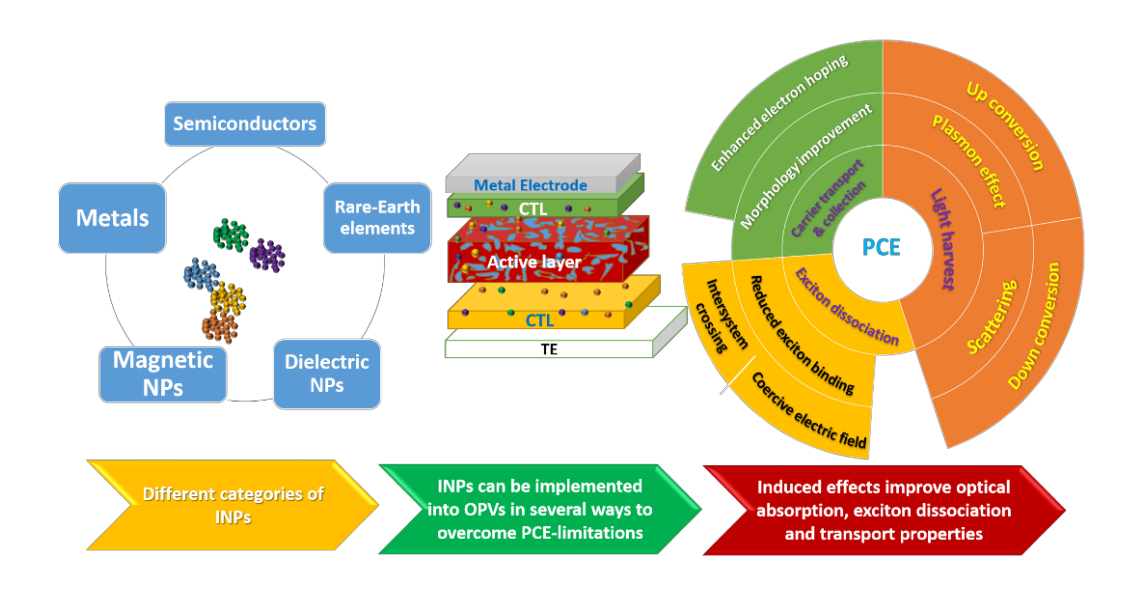
<sup>b</sup> Physics Department, Faculty of Science, Minia University, P.O. Box 61519 Minia, Egypt

<sup>c</sup> Medical Physics Department, College of Medical Sciences Techniques, The University of Mashreq, Baghdad, Iraq <sup>d</sup> Hochschule Fresenius gGmbH-University of Applied Science, Faculty of Chemistry and Biology, D-65510, Idstein, Germany.

# **Abstract**

Organic photovoltaics (OPVs) have received considerable attention over the past two decades as a promising alternative to their inorganic counterparts. Although the power conversion efficiency (PCE) of OPVs has rapidly increased in the last ten years exceeding 18%, higher PCEs are still needed to commercialize this emerging technology. The weak light absorption, particularly at wavelengths outside the visible region, and the recombination losses of the photo-generated charge carriers represent the major challenges for the PCE of OPVS. The light harvest and survival of the photogenerated charge carriers within OPVs are restricted to multiple factors such as material properties and device engineering. The application of different types of inorganic nanoparticles (INPs) in OPVs has been reported by many researchers as an effective strategy to overcome most of the PCE-limitations. Here, a comprehensive overview of the progress in the performance of OPVs due to the application of different INPs over the past decade is provided. This review also presents an in-depth analysis of the efficiency loss pathways at the different steps of the photovoltaic effect and how INPs can address these issues resulting in PCE enhancement of OPVs. Finally, the impacts of this approach on the stability and cost of the device in addition to challenges and outlook are discussed.

# **Graphical Abstract**



# **Keywords:**

Organic photovoltaics – Inorganic nanoparticles – exciton dissociation – carrier mobility – carrier recombination- Up and down conversion of light.

# **Table of Contents**

1. Introduction	2
2. Efficiency limitations of BHJ organic solar cells	
3. INPs for OPVs	θ
3.1. Metal nanoparticles	7
3.1.1. Localised surface Plasmon resonance (LSPR)	7
3.1.2. Noble Metal nanoparticles	8
3.1.3. Low-cost metal NPs	12
3.2. Dielectric NPs	13
3.2.1. Improved dissociation of excitons	13
3.2.2. Enhanced light absorption	15
3.3. Semiconducting NPs	16
3.3.1 Enhanced morphology	16
3.3.2. Improved carrier hoping	20
3.4. Magnetic NPs	21
3.4.1. Intersystem crossing.	21
3.4.2. Coercive electric field	22
3.5. Rare-Earth elements NPs	24
3.5.1. Up conversion nanoparticles (UC NPs)	25
3.5.2. Down conversion (DC) nanoparticles	30
4. Preparation methods of INPs-based OSCs	32
5. The impact of different types of INPs on the lifetime and cost of OPVs	33
6. Summary and perspectives	33
Acknowledgement	34
References	31

#### 1. Introduction

Over the past two decades, organic photovoltaics (OPVs) have shown promising potential as a third-generation PV technology, due to their low production cost, abundance of materials, and mechanical flexibility [1-4]. The power conversion efficiency (PCE) of bulk heterojunction (BHJ) OPVs has recently exceeded 18% [5-7] for mono-layer devices achieving an improvement of ~150% over the past ten years [8]. However, higher PCEs are still needed before large scale commercialization of this promising technology (OPVs) [9, 10]. The photoactive layer of a typical BHJ OPV device is comprised

of an electron donor (D) blended with an electron acceptor (A) in a continuous interpenetrating network. When incident sunlight is absorbed by the active layer, an exciton (a bound state of electronhole pair) is generated which diffuses towards the D/A interface to be dissociated into free holes and electrons, which transport through the D and A phases to be collected at the anode and the cathode, respectively, to produce a photocurrent [11-14]. The limited light harvest and the high carrier recombination losses are the main limitations of the PCE of OPVs [15-17] as will be discussed in more detail in section 2.

The solar spectrum received by the Earth's surface consists of infra-red (IR) radiation (52%), visible light (43%) and the remaining 5% lies within the ultraviolet (UV) region [18]. The portion of the solar spectrum that can be harvested by OPVs depends on the energy gap ( $E_g$ ) of both donor and acceptor materials. Only photons with energy  $\ge E_g$  of the donor or the acceptor can be absorbed and generate excitons. The lower the band gap, the higher is the portion of the solar spectrum that can be harvested by the device. The state-of-art light harvesting materials in OPVs can absorb within a narrow region, mainly the visible light, of the solar spectrum [19]. Furthermore, the number of photons absorbed by the device at a particular wavelength increases with increasing the active layer thickness. On the other hand, a narrow bandgap can lower the open circuit voltage ( $V_{OC}$ ) and, consequently, the PCE of the device. Moreover, a thick active layer increases charge carrier recombination as a result of the short diffusion length and short lifetime of the photo-generated excitons [20-22]. Thus, a trade-off between optical absorption and both  $V_{OC}$  and carrier transport should be reached for optimum performance [23].

Different strategies were proposed over the past decades to enhance the efficiency of OPVs. Performance improvement can occur either through the development of efficient materials or employing approaches that can optimize the device structure and engineering. For instance, the development of low bandgap conjugated donor polymers [24-26] as well as tunable non fullerene (NF) acceptors [27] have greatly improved the PCE of OPVs by increasing the harvest of light by the device. Thermal and solvent annealing processes as well as the utilization of solvent additives can improve the crystallinity and morphology of the active layer of the device [28-30]. Plasma treatment was reported as a good approach to enhance the morphology and electronic structure of the active layer [31] and charge transport layers [32, 33] of OPV devices. The concept of ternary devices which use an additional third component, either donor or acceptor, has been a successful approach towards better performance OPVs [34-41]. The incorporation of different types of inorganic nanoparticle (INPs) into the active layer and /or the buffer layer(s) of OPVs has likewise shown a great potential to increase light absorption and reduce carrier recombination within the device.

Several attempts to improve the efficiency of OSCs via the incorporation of various categories of INPs within the photoactive layer as well as charge transport layers were reported in the last decade. For instance, metal nanoparticles such as silver and gold have shown a great potential to improve the device performance through increasing light absorption and carrier mobility within the device [42]. Moreover, other types of INPs such as dielectrics were employed to enhance the dissociation of the photo-generated exciton [43]. The application of magnetic NPs e.g.  $Fe_3O_4$  was found to increase the lifetimes of the generated excitons, which as a result significantly reduces their recombination rate [44]. In addition, semiconductor NPs such as CuO,  $Cr_2O_3$  and CuC have demonstrated to reduce the carrier recombination through improving the morphology of the doped layer, which enhances the transport properties of the device [45-47].

It has been reported that the bandgap of the donor polymer should range from 1.5 to 1.8 eV, corresponding to absorption of near infrared and visible regions of the solar spectrum, to achieve a balance between light absorption and  $V_{OC}$  [48]. Therefore, a large portion of the solar spectrum (sub-

bandgap) photons incident on OPVs are lost through transmission without generating a photocurrent. The employment of up-conversion (UC) NPs such as Lanthanide ions in OPVs has been recently reported by many researchers. UC NPs are added to the device structure with the purpose of increasing the light harvest of the device via the conversion of low energy photons such as from the IR range into higher energy photons, mainly in the visible region, which correspond to the bandgap of most of the donor materials. On the other hand, photons with much higher energies than Eg of the absorber material will dissipate part of their energy into heat. Moreover, ultraviolet (UV) radiation can induce changes in the structure of organic materials through photo-oxidation reactions leading to the degradation of the device [49]. Therefore, the utilization of down-conversion (DC) NPs in OPVs can enhance the optical absorption and stability of the device due to converting such high energy photons into visible light.

In this review, the implementation of the different categories of INPs, including metal, semiconductor, dielectric, ferromagnetic, and up and down conversion NPs, for OPVs will be discussed comprehensively. The different mechanisms in which such NPs can affect the operation of OSCs will be described in detail. In addition, the progress in device performance over the past decade, achieved by dopant NPs of different categories, will be reviewed. The impact of the application of INPs in OPVs on the lifetime and the cost of the device is discussed. Finally, conclusions and outlooks are presented for future research. A brief discussion on the limiting factors to the PCE of BHJ OPVs is given first to deeply understand how different INPs can have positive impacts on the device performance.

# 2. Efficiency limitations of BHJ organic solar cells

An in-depth insight on the structure and operation of BHJ OPVs is necessary to form a comprehensive understanding of the limitations to their performance. The BHJ structure was developed by Yu *et al.* [50] in 1995. The active layer was composed of two organic semiconductors: one acts as an electron donor that mainly absorbs sunlight while the other functions as an electron acceptor, in a blend film between to dissimilar electrodes. Later, buffer layers have been introduced between the electrodes and the active layer known as electron and hole transport layers (ETL) and (HTL), respectively, to facilitate charge collection at the electrodes. The BHJ structure offers continuous networks within the active layer that are needed for charge dissociation and collection. The length of these D/A domain interfaces should be within the range of the diffusion length of the exciton. The BHJ structure can be produced in an either regular geometry, where the transparent electrode works as an anode, or an inverted geometry in which a transparent electrode is the cathode, as shown in Fig.1.

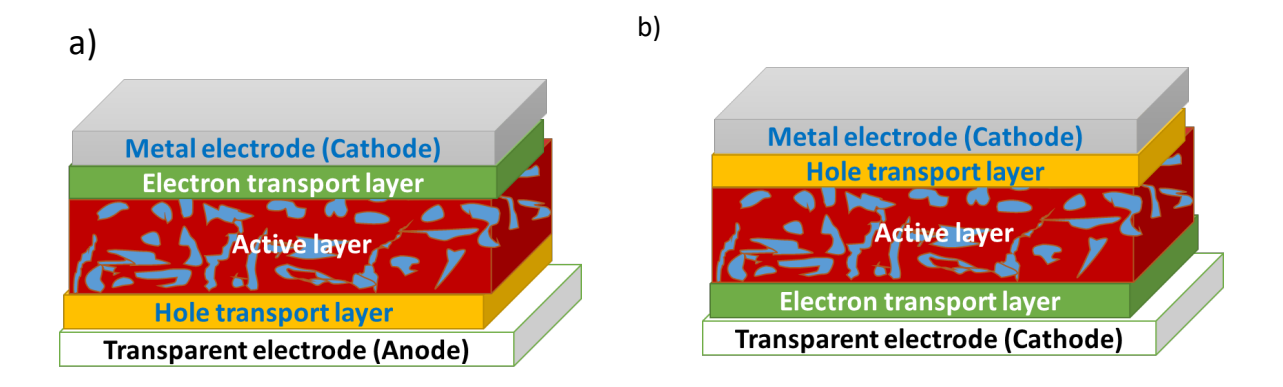


Fig. 1. (a) Regular (b) Inverted geometry BHJ structures of OPVs.

In OSCs, the photovoltaic (PV) effect, i.e. the generation of electric voltage at the interface of two different materials as a result of light absorption [51], can be divided into five consequent steps (Fig. 2). Firstly, a photon with energy  $\geq E_g$  of the donor/acceptor is absorbed by one of the bonding electrons within the high occupied molecular orbital (HOMO) and is excited to the lowest unoccupied molecular orbital (LUMO), leaving an empty state (hole) behind. The low dielectric constant of organic semiconductors causes the photo-generated electron-hole pair to be strongly bound by electrostatic attraction, known as excitons. Excitons then diffuse within their diffusion length ( $L_D$ ) towards the (D/A) interface where exciton-dissociation into free charge carriers occurs due to the energy offset between their LUMOs, which can provide the energy required to overcome the binding force of the exciton. For other structures such as layer-by-layer (LBL) OPVs, excitons can transfer their energies from the donor to the acceptor at the D/A interface through energy transfer resulting in improved PCEs [52]. Subsequently, the free electrons are transported through the acceptor material and the holes through the donor, and are finally collected at the respective electrodes to produce a photocurrent at the external circuit [13, 14, 53].

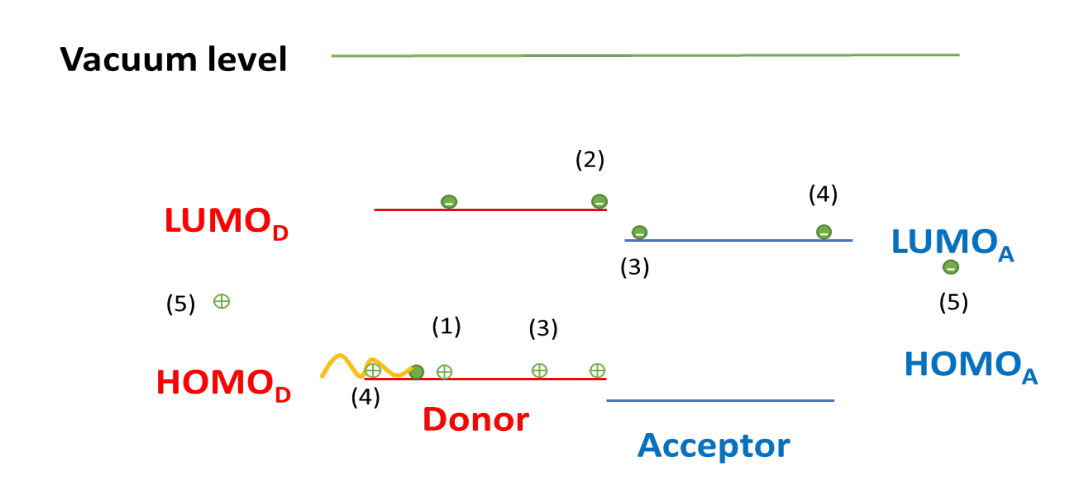


Fig. 2. Schematic representation to the steps of PV effect in organic solar cells. 1: light absorption and generation of exciton. 2: diffusion of exciton. 3: Exciton dissociation at the D/A interface. 4: Transport of free carriers. 5: charge collection at the respective electrodes.

The external quantum efficiency (EQE) and hence PCE of OPVs depend on the yield of the aforementioned five steps and can be calculated according to the following equation [54].

$$EQE(\lambda) = \eta_{abs.} * \eta_{diff.} * \eta_{diss.} * \eta_{tr.} * \eta_{coll.}$$
(1)

Where  $EQE(\lambda)$  represents the ratio between the number of photoelectrons collected by the device and the number of incident photons at a particular wavelength.  $\eta$  is the efficiency of each process as depicted by the subscript as discussed above.  $EQE(\lambda)$  is related to the PCE through the spectral photon flux,  $\Phi_{Ph,\lambda}^{AM1.5}$  as follows [51]:

$$J_{SC} = -q \int_{\lambda_1}^{\lambda_2} EQE(\lambda) \, \Phi_{Ph,\lambda}^{AM1.5} d\lambda \tag{2}$$

$$PCE = \frac{J_{SC} * V_{OC} * FF}{P_i} \tag{3}$$

FF and  $P_i$  are the fill factor and the incident power, respectively. According to the abovementioned discussion and Eq. (1), the limitations to the efficiency of an OPV device can be summarized as below:

- i. The limited light absorption due to the spectral mismatch between the incident solar spectrum and the optical absorption of the constituents of the active layer. The optimum bandgap of the light harvesting materials for OPVs was found to be in the range of 1.5 to 1.8 eV [48] to avoid losses in the V<sub>OC</sub>. In addition, the small thickness (100-200 nm) of the active layer reduces the intensity of the absorbed light. Although thicker films can absorb more light, this approach will lead to a decreased performance of OPVs due to increased carrier recombination loss.
- ii. The low exciton diffusion as a result of the short L<sub>D</sub> and lifetime of the photo-generated excitons in the range of 20 nm and <1 ns for singlet excitons formed within the majority of conjugated polymer films [55]. Therefore, only excitons generated close to the D/A interface can be dissociated into free charge carriers. In addition, the built-in electric field (E<sub>bi</sub>) of OPVs is not sufficient to sweep (drift) all the generated excitons out towards the D/A interface before they recombine [56, 57].
- iii. The high binding energy of the photo-generated excitons due to the low electric permittivity of the active blend results in energy loss and reduced  $V_{OC}$  and hence, the PCE of the device decreases.
- iv. The poor and imbalanced carrier mobility associated with morphology imperfections and low crystallinity of the active layer constituents negatively affect carrier transport, leading to non-geminate recombination before collection at the relevant electrodes [58].
- v. Losses due to series and shunt resistances (R<sub>s</sub> and R<sub>sh</sub>), where R<sub>s</sub> is ascribed to the resistance of the bulk semiconductor, electrodes and the contact between them, while R<sub>sh</sub> describes the leakage photocurrent through the defects within the junction or at edges of the cell, which act as alternative paths to the photo-generated electrons. Thus, a high R<sub>s</sub> and low R<sub>sh</sub> result in weak carrier collection.

Consequently, improving the performance of OPVs requires enhancing the efficiency of at least one of the five processes described in Eq. (1). This enhancement can be achieved in several ways such as material development and device engineering. INPs have shown a great potential to overcome all the aforementioned limitations. In the following sections, different categories of INPs that can enhance the performance of OPVs are discussed in detail.

## 3. INPs for OPVs

Over the past decade, a significant enhancement in the PCE of OPVs was reported due to the development and implementation of effective materials for the different layers of the BHJ OPVs. Moreover, many strategies were developed that can be applied to most organic solar cells (OSCs) with different structures and materials. These strategies, in addition to the developed materials, maximize the conversion efficiency of the device. One of these remarkable methods is based on the utilization of inorganic nanoparticles within the photoactive and/or buffer layers of the device. Based on the type, shape, and size of the dopant NPs, their properties as well as their impact on the device performance can vary significantly. Therefore, different approaches to improve the overall performance of OPVs were reached based on the employment of various dopant INPs. In the following sections of this review, outstanding findings achieved as a result of dopant NPs for OPVs as well as the

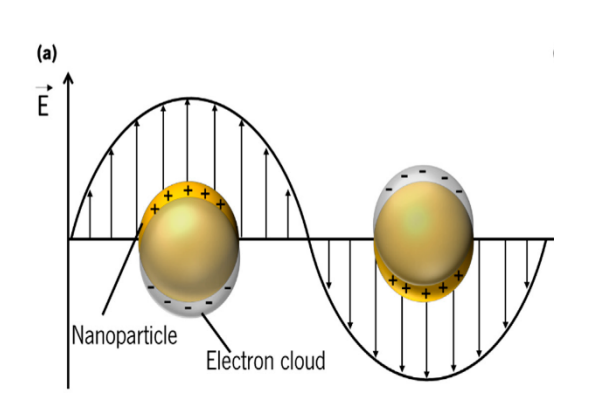
physics and performance-enhancement mechanisms behind each type of dopant INPs will be discussed in detail.

#### 3.1. Metal nanoparticles

The utilization of metal nanoparticles (MNPs) in OPVs aims mainly at increasing the absorption of light by the active layer via localized surface Plasmon resonance (LSPR) effect. LSPR describes the interaction between the incident light and the oscillating conduction electrons on the surface of MNPs, which leads to selective attenuation of light in addition to an enhanced electromagnetic field close to the surface of the MNPs. Furthermore, MNPs can lead to either forward or backward scattering of the incident light. Therefore, the application of MNPs in OPVs represents an excellent strategy to enhance optical absorption and hence the number of the photo-generated excitons by the active layer. In the following, the implementation of both noble metals NPs and low-cost MNPs will be discussed.

# 3.1.1. Localised surface Plasmon resonance (LSPR)

When the oscillating electric field of the incident light hits the surface of MNPs, it causes the conduction electrons to displace relative to the nuclei. Due to the electrostatic attraction between the opposite charges of the electrons and nuclei, a restoring force arises which leads the electron cloud to oscillate coherently with the incident electric field (Fig. 3) [59]. The oscillation frequency ( $\omega_p$ ) depends on the dimensions and shape of the NPs as well as the dielectric medium [60]. The collective oscillation of the conduction electrons is known as localised surface Plasmon resonance (LSPR). When light is incident at the resonance frequency  $(\omega_p)$ , the surface plasmons (quantized oscillating plasma) are excited to higher states upon the absorption of radiation leading to enhanced electric field close to the surface of MNPs. The excited surface plasmons subsequently decays through reemission/scattering of light [61, 62]. Thus, the existence of such MNPs within the structure of OPVs helps to improve the light harvest as well as the generation of excitons. The resonant frequency  $(\mathbb{D}_p)$ can be controlled by the size, geometry and the type of NPs. Thus, dopant MNPs should be selected carefully so that their plasmonic resonance frequency is close to the bandgap of the donor polymer and hence, light harvest can be improved. Typical absorption spectra of plasmonic Ag NPs are shown in Fig. 3(b). The absorption peak broadens and notably shifts towards longer wavelengths (red-shift) as the particle diameter increases [42].



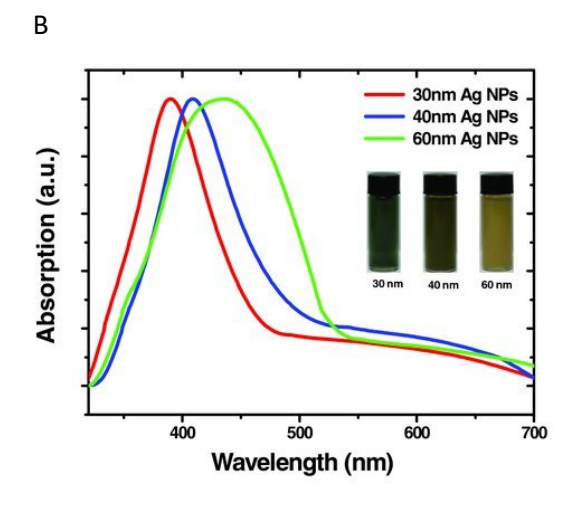


Fig. 3. (a) Representation of the localized surface plasmon on nanoparticles (b) The variation of absorption spectra of Ag NPs with the particle size [42].

Enhancement of the PCE of OPVs by plasmonic NPs is achieved by two main effects: namely far-field scattering and near-field effect. The scattering of the incident sunlight by MNPs embedded into the different layers of an OPV device plays a crucial role in improving its absorption through increasing the length of the optical path within the device. Due to the LSPR effect, the strength of the electromagnetic field surrounding the surface of MNPs, within few nanometres distance, increases light absorption. For the near-field to be effective in the photo-generation of exciton, MNPs must be embedded into or close to the photoactive layer, while the far-field scattering can improve the light absorption either when MNPs are inside or outside the photoactive layer. MNPs can be located in front, rear or within the photoactive layer. The direction of light scattering generally depends on the particle size. For example, it was found that the forward scattering for Ag NPs increases with particle size up to 67 nm and that backward scattering increased at larger particle size [63]. Forward scattering is essential when the MNPs are embedded into the front charge transport layer: namely HTL and ETL for regular and inverted geometry, respectively.

The addition of plasmonic NPs to the rear buffer layer typically enhances light trapping within the active layer of the device. This approach increases optical path length as photons backscatter from the surface of MNPs and hence absorption probability increases. Although the light scattering by MNPs improves with large particle size, it was reported that large MNPs (>60 nm) negatively affect the photovoltaic performance through significant parasitic absorption as well as shunting and morphology issues [64]. In addition, further loss mechanisms are possible with plasmonic NPs of small size (<20 nm), which can act as recombination centres for the photo-generated charge carriers and hence reduce the photocurrent and the PCE of the device [65, 66]. Therefore, the size of MNPs should be selected precisely for optimum performance.

#### 3.1.2. Noble Metal nanoparticles

The incorporation of noble metals NPs such as silver (Ag) and gold (Au) in OPVs was early reported by many researchers. The enhancement of the PCE of OPVs due to the LSPR effect is mainly attributed to the improved J<sub>SC</sub> caused by increased light absorption, while both FF and V<sub>OC</sub> remain almost unchanged. It is worth to mention that adding noble MNPs such as (Ag) and (Au) with small particle size (5-6 nm) and in low concentrations into OPVs was found to significantly increase all the photovoltaic parameters (including FF and Voc), which cannot be explained based on LSPR alone. For instance, in 2005 Kim and Carroll [67] have recorded 50-70% enhancement in the PCE of poly (3octylthiophine) (P3OT):C60-based BHJ OPVs due to Ag and Au dopants with the maximum improvement in PCE with Ag NPs. The observed progress was attributed to the improved electrical conductivity of the active blend through providing energy levels of the doping material within the bandgap of the donor polymer and the reduced  $R_s$  (from 46 to 15  $\Omega$  cm<sup>2</sup>) of the device, with little increase in light absorption. Wang et al.[42] investigated the influence of larger sizes (30, 40 and 60 nm) and controlled shape of Ag NPs on the performance of PCDTBT: PC<sub>70</sub>BM based OSCs. Their best device with 40 nm Ag NPs exhibited a higher PCE of 7.1% compared to that of the reference device (6.3%). The introduction of Ag NPs into the donor/acceptor blend enhanced the light absorption and charge transport and hence resulted in higher J<sub>SC</sub> (from 10.79 to 11.61 mA/cm<sup>2</sup>) and a slight change in FF (0.68 to 0.69) and EQE were obtained. The efficiency enhancement varied significantly between ref. [42], which had an almost 13% improvement, and devices in [67] that exhibited an up to 70% increase with respect to their control devices. This variation can be assigned to the different active layers, device structure and particle size. The different HOMO levels of both donor polymers with

respect to the fermi level of Ag NPs may impact the hole transfer through the device. In addition, any possible aggregations in case of larger NPs can hinder carrier transfer and act as recombination centres. Therefore, all the previous parameters need to be considered to achieve the best benefit from this performance-enhancement strategy. In the same context, Wang and co-workers [68] investigated the effect of Au truncated octahedral NPs (~70 nm) on three different OSCs. The three devices were based on P3HT, PCDTBT and Si-PCPDTBT as electron donors, while PC<sub>70</sub>BM was used as acceptor (Fig. 4). The PCE of all devices in this study showed enhanced photovoltaic parameters as a result of stronger light absorption as well as reduced R<sub>s</sub> and increased R<sub>sh</sub>. Moreover, the reflection of the incident light by Au NPs increased the path length of photons within the active layer, which increased the absorption of light. Their results were also confirmed by dark J-V measurements, which revealed a lower leakage current in case of NPs-based BHJ devices.

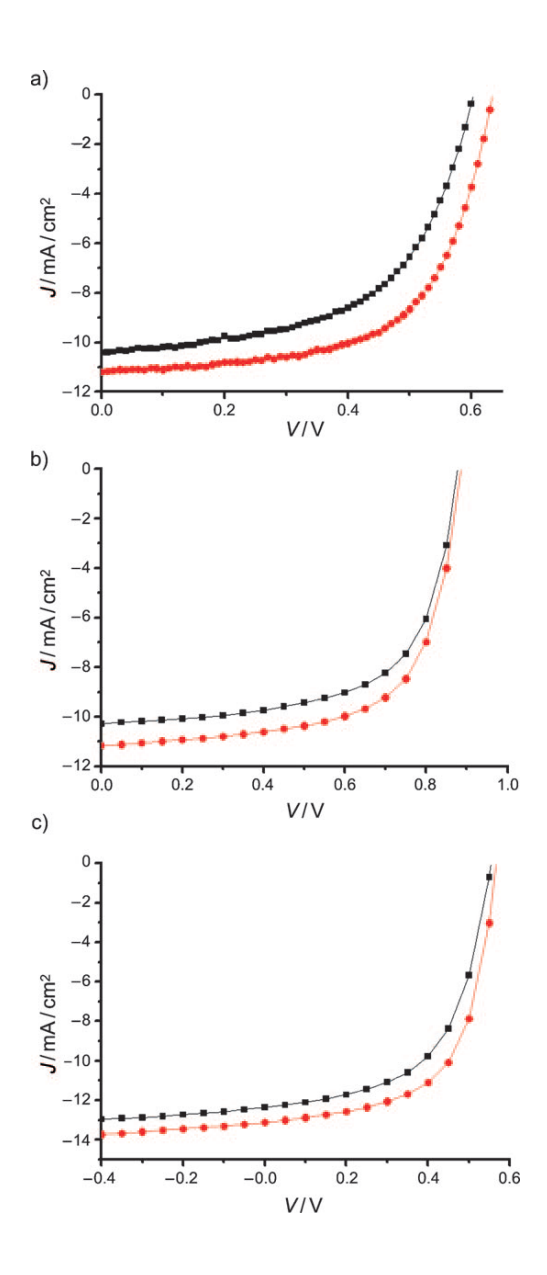


Fig. 4. J–V curves of devices with plain BHJ (black curves) or BHJ with 5 wt% Au nanoparticles (red curves) depending on photovoltaic materials (a) P3HT/PC70BM BHJ (ca. 220 nm) (b) PCDTBT/PC70BM BHJ (ca. 120 nm), and (c) Si-PCPDTBT/PC70BM BHJ (ca. 150 nm) [68].

More interestingly, the addition of MNPs into the BHJ active blend not only improves the PCE of OPVs, but also enhances their durability under operating conditions. Paci *et al.* [69] investigated the impact of Ag NPs on both, the efficiency and stability of the device. Ag NPs were incorporated into a P3HT: PCBM active layer to produce a plasmonic OPV device. Improvement in the PCE of the device was observed because of the LSPR effect, as discussed above. Additionally, the stability of the Ag NPs-doped device upon continuous illumination was also enhanced in comparison with the control device. The improved durability was attributed to the more stable morphology in case of doped active layer with little aging impact at the interface with HTL. Contrarily, the Ag-free counterpart revealed significant aging effects as well as morphological changes during illumination leading to a thicker layer with time. A more comprehensive discussion on how MNPs improve the device stability is given elsewhere in this review (section 5).

Remarkable improvements in the performance of OPVs were also achieved through the introduction of MNPs into other locations of the device such as ETL, HTL or between buffer layers and the active layer. For instance, adding Au NPs to the HTL was found to increase exciton generation rate with higher dissociation probability due to LSPR [70]. Moreover, Spyropoulos *et al.* [71] reported the influence of the deposition of Au and Ag NPs on the top of PEDOT: PSS HTL,which led to 20% enhancement in the cell's efficiency. Their results confirmed that the introduction of MNPs as an interlayer between the active layer and HTL can also exploit the advantages of LSPR by increasing light harvesting and hence resulting in a better performance. The utilization of Ag NPs in both buffer layers has also proven an effective strategy to increase the efficiency of OPVs [72]. Au NPs were incorporated into HTL and ETL, which led to a 13% increase in the PCE of the device due to dual plasmonic resonance that increased light trapping.

The incorporation of MNPs into buffer layers does not always improve the optical absorption of the plasmonic device. This is decided based on the orientation of the LSPR-resulting field, either laterally or vertically. Lateral orientation of the resonance field leads to weak absorption as less amount of light can reach the active layer in contrast to vertical orientation. However, MNP-doped buffer layers can show improved morphologies with increased surface roughness, which subsequently increases the area of contact with the active layer resulting in an efficient carrier collection and a lower R<sub>s</sub>. The aforementioned effects were confirmed by Xie and co-workers who studied the influence of Au NPs doping of the active layer and HTL of a P3HT: PCBM-based device. The impact of Au NPs was studied individually on HTL, the active layer and simultaneously on both layers as shown in Fig. 5. An increase of 22% in PCE was observed for the device with Au NPs dopant in both layers with respect to the reference device due to simultaneously improved optical and electrical properties [73].

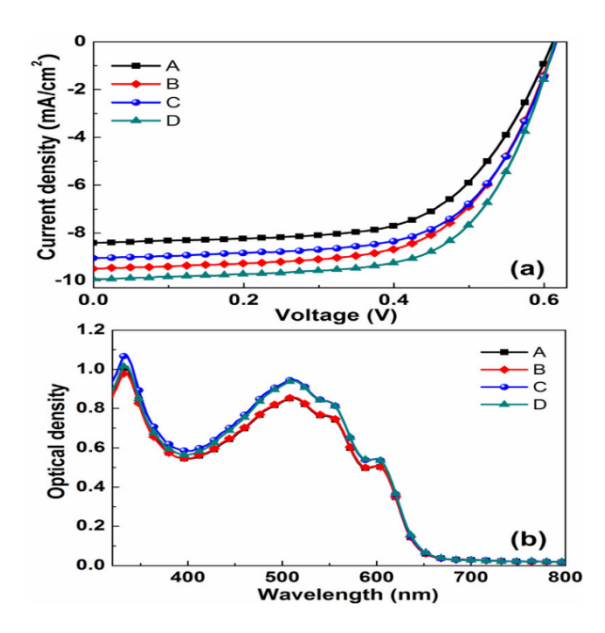


Fig. 5. (Color online) (a) J-V characteristics of the PSCs with NPs incorporated into different layers under AM 1.5G illumination at 100 mW/cm2. (b) Absorbance of the active layer for different NP doping structures. (Device A: No NPs; B: NPs in PEDOT: PSS only; C: NPs in P3HT: PCBM only; and D: NPs in both P3HT: PCBM and PEDOT: PSS) [73].

Different approaches were developed for the best use of noble MNPs in OPVs such as the addition of Au NPs into the photoactive blend with the fabrication of Ag nano-grating. This design had an improved light absorption and electrical properties leading to enhanced PCE [74]. Another effective strategy to enhance the device efficiency was proposed by incorporating both Ag and Au NPs into the HTL and the active layer [75-77]. An improvement of ~20% in the conversion efficiency of the device was reached with this method. The dual plasmonic effect led to increased harvesting of light and EQE. In addition, the improved hole collection contributed to the overall efficient device performance [75].

Further studies focusing on the influence of size, concentration and the shape of nano dopants on device performance were conducted. The impact of the size of NPs incorporated into different layers of OPVs was investigated by many groups [78, 79]. For example, Ag NPs with variant sizes incorporated within the PEDOT: PSS buffer layer have been reported [78]. It was shown that the scattering of light towards the active layer can be controlled by the size of MNPs. An optimum efficiency of the devices was recorded with Ag NPs of ~67 nm size. Results revealed that the enhancement in PCE of the devices is ascribed only to the increased light absorption due to scattering by Au NPs. In addition, the effect of inserting differently shaped nanomaterials, either into the buffer layers or the active blend of OPVs, was reported by many groups [80-83]. For instance, Li and coworkers used Ag NPs and nanoprisms as dopants to the active layer. LSPR varied with the shape of the nanomaterial used within the photoactive blend (Fig. 6). The absorption of light by the device was broadened and hence an increased EQE and PCE were reached [80]. Improved J<sub>SC</sub> and PCE were recorded with Au nanorods incorporated into PCDTPT: PC<sub>71</sub>BM active layer due to LSPR [84].

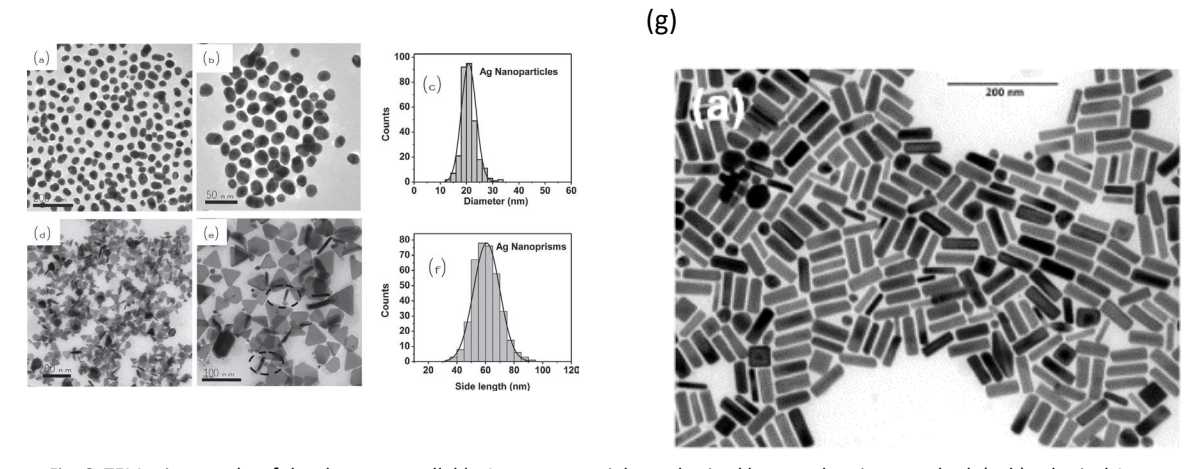


Fig. 6. TEM micrographs of the shape-controllable Ag nanomaterials synthesized by wet-chemistry method: (a, b) spherical Ag nanoparticles; and (d, e) triangular Ag nanoprisms. (c, f)Size-distribution histogram of the as-prepared Ag nanoparticles and Ag nanoprisms, respectively. In (e), it should be noted that the 'rod'-shaped Ag nanomaterials in the TEM marked by black circles are not nanorods but are vertically oriented nanoprisms [80]. In (g) TEM image for Au nanorods reproduced from [84].

#### 3.1.3. Low-cost metal NPs

Cost-effective MNPs such as copper (Cu) and aluminium (Al) were also proposed to increase the efficiency and stability of OPVs [85-87]. For example, the impact of copper (Cu) NPs (~20 nm) on the optical and electrical properties of P3HT film was studied by Szeremeta et al. [85]. Cu NPs strongly improved the photocurrent of the polymer without significant changes to its absorption spectrum. The incorporation of Cu NPs into the polymer matrix was found to enhance the dissociation of excitons through the interaction of the plasmonic field with excitons. This field subsequently facilitates exciton transfer through the polymer matrix and hence reduces geminate recombination. Overall, Cu NPs showed promising potential towards more efficient OPVs. Additionally, Cu NPs were incorporated in Tungsten Oxide (WO<sub>3</sub>) HTL via thermal evaporation, where an ultra-thin layer (up to 4 nm) of Cu was deposited (WO<sub>3</sub>/Cu/WO<sub>3</sub>). The device with Cu NPs exhibited an enhanced PCE of 6.38% compared to the control device with a PCE of 4.65% due to LSPR that increased light harvest and hence J<sub>SC</sub>, as confirmed by EQE and UV-VIS data (as shown in Fig. 7 and Fig. 8) [88].

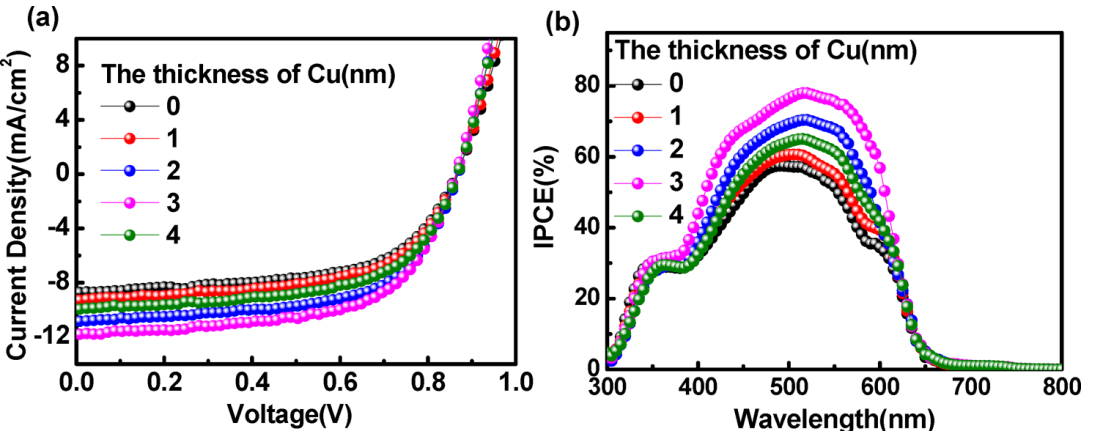


Fig. 7. (a) J–V characteristics of devices with different thicknesses of Cu NPs under 100 mW cm<sup>-2</sup> simulated AM1.5G in ambient air (b) Incident photon to current efficiency (IPCE), same as EQE, characteristics of devices with different thicknesses of Cu NPs [88].

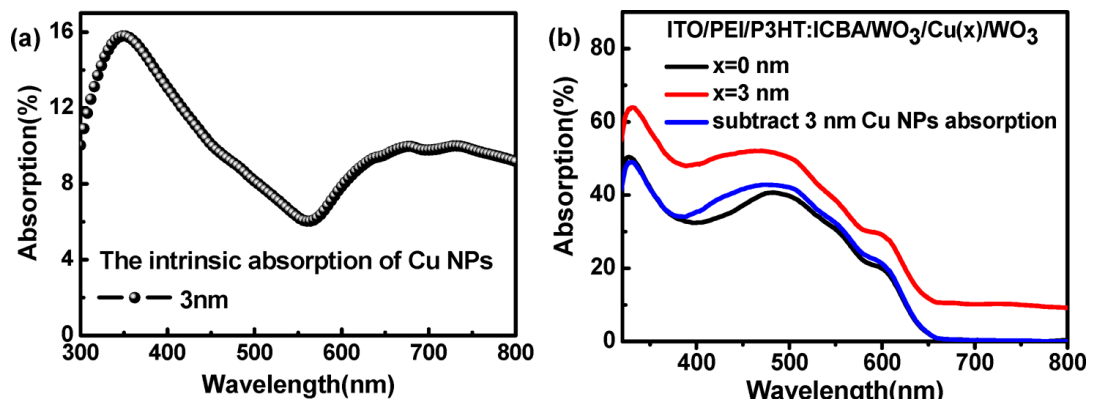


Fig. 8. (a) UV-vis intrinsic absorption spectra of 3 nm Cu NPs (b) absorption spectra of devices with 0 and 3 nm thicknesses of Cu NPs without the top electrode in the wavelength range from 320 to 800 nm, and absorption of a device with 3 nm Cu NPs, which subtracted the intrinsic absorption of 3 nm Cu NPs [88].

Moreover, Cu-Au NP blends were added into PEDOT: PSS HTL of three devices with different active layers, P3HT: PC<sub>61</sub>BM, PTB7-Th: PC<sub>61</sub>BM and PTB7-Th: PC<sub>71</sub>BM. An improvement in PCE of up to 13.4% was achieved with a maximum PCE of 8.48% due to the enhanced plasmonic effect over a broader spectrum [89]. Similar to noble MNPs, the low cost MNPs have been shown to improve the lifetime of the OPVs due to their ability to stabilize the morphology of the active layer and its interface with the metal electrode. In this context, Al NPs with average sizes of 30 nm were added to the active blend consisting of P3HT: PCBM. Subsequent results revealed a better morphology and stronger light absorption for the doped device than for the reference counterpart, especially at shorter wavelengths, as confirmed by EQE data leading to higher PCE. In addition, a longer lifetime (5-times longer than the non-doped device and twice that based on Au NPs) was realized with a plasmonic device as a result of its stable morphology, depressing photo-oxidation of the donor polymer [86]. More details on such stability-enhancement mechanisms are discussed in section 4 of this review.

Recently, multiple plasmonic NPs were added simultaneously to the active layer. A three-metal nanocomposite based on Ag, Zn and Nickel (Ni) NPs was blended with a PTB7: PCBM active layer in an inverted OPV device. The efficiency of the doped device increased by  $^{\sim}25\%$  compared to the non-doped (control) counterpart. The recorded improvement was attributed to the LSPR by MNPs as well as a better morphology and enhanced crystallinity [90]. Furthermore, a remarkable improvement in PCE exceeding 47% was achieved by magnesium (Mg) NPs added to tin dioxide (SnO<sub>2</sub>) ETL in an inverted device based on P3HT: PCBM [91]. The incorporation of Mg NPs significantly improved the electrical properties of the device leading to increased electron mobility,  $R_{SH}$  and reduced  $R_{S}$ .

#### 3.2. Dielectric NPs

#### 3.2.1. Improved dissociation of excitons

Non-plasmonic NPs, such as those with high dielectric constants, were used as dopants to improve the performance of OPVs. The interaction of light with organic semiconductors comprising the active layer of OPVs is quite different from their inorganic counterparts such as Si, Ge, CdTe, etc. In inorganic semiconductors, the absorption of light results in free charge carriers (electrons and holes), while for organic semiconductors, the generated electron-hole pairs are still bound to each other via Coulomb attraction due to the low dielectric constant of such materials [92]. According to Coulomb's law, the lower the dielectric constant of the medium, the stronger the electrostatic attraction force between

the electron and the hole. The exciton dissociation rate,  $K_D$  (E), at the D/A interface can be given according to Onsager's theory [93].

$$K_D(E) = K_R \frac{3}{4\pi a^3} e^{\frac{-E_B}{K_B T}} \left[ 1 + b + \frac{b^2}{3} + \frac{b^3}{18} + \frac{b^4}{180} + \cdots \right]$$
 (4)

Where a is the electron-hole pair distance,  $E_B$  is the exciton binding energy,  $K_B$  is Boltzmann's constant and T stands for the absolute temperature in Kelvin.

$$b = \frac{q^3 E}{8\pi \varepsilon K^2_R T^2} \tag{5}$$

 $K_R$  is Langevin recombination and can be expressed as: [92, 94]

$$K_R = -\frac{q}{\varepsilon} \min(\mu_e, \mu_h) \tag{6}$$

Where q is the electron charge and  $\mu_e$ ,  $\mu_h$  are the mobility of the electron and hole, respectively.

These bound state electron-hole pairs (excitons) need to be dissociated prior to charge collection at the electrodes. Exciton separation occurs at the interface between the donor and the acceptor due to the offset between their LUMO levels. This energy lost in the dissociation of excitons is directly reflected on the value of  $V_{OC}$  of the device. The value of  $V_{OC}$ , for many donor: acceptor (fullerene) systems, was found to relate to the HOMO and LUMO levels of the donor and acceptor, respectively, as: [48, 95]

$$V_{OC} = \frac{1}{a} \left( E_{Donor}^{HOMO} - E_{Acceptor}^{LUMO} \right) - 0.3 \tag{7}$$

Thus, according to Eq. (7) and Fig. 2, when the difference between the LUMO levels of the donor and the acceptor is significant, exciton dissociation is easier. The difference between the LUMO levels of the donor and acceptor can be designed through the following means:

- i. Selecting a donor polymer with elevated HOMO and LUMO with respect to the acceptor. However, in this case, the donor HOMO will move closer to the acceptor LUMO, dramatically decreasing  $V_{\text{OC}}$  and hence PCE.
- ii. Selecting a donor polymer with a high LUMO, while the HOMO is still low with respect to the LUMO of the acceptor. In this case, the optical bandgap of the donor increases, which reduces the light absorption of the polymer, J<sub>SC</sub> and the PCE of the device.
- iii. Developing an acceptor with relatively low LUMO, but this strategy will lead to drops in VOC and PCE of the device as the difference between E<sub>HOMO, Donor</sub> and E<sub>LUMO, Acceptor</sub> decreases.

Thus, it is necessary to find effective approaches to improve the separation of excitons without disturbing the photovoltaic parameters of the device. Consequently, NPs with high electric permittivity were used as dopants to increase the electric permittivity of the whole medium (active layer), which reduces the binding energy of the excitons and hence facilitates their separation into free carriers. For instance, barium and strontium titanate (BaTiO<sub>3</sub> & SrTiO<sub>3</sub>) NPs were used to increase the dielectric constant of the active blend composite and resulted in significant improvement in the PCE of the device, especially with SrTiO<sub>3</sub>. The increased efficiency was attributed to the improved dissociation of excitons and an increased yield of light harvesting [43, 96].

In contrast, the high dielectric constant of such NPs can increase the series resistance of the device which causes the device performance to drop. The distribution of the NPs within the active layer is a critical aspect that needs to be highlighted. The degree of enhancement of the device performance strongly depends on how the NPs are embedded within the doped layer. Large agglomerations of the NPs show a negative impact on the charge transport and collection, which can eventually lead to a decline in the performance of the OPVs. This was confirmed in ref. [43, 96] where both J<sub>SC</sub> and PCE of the devices doped with the high dielectric constant NPs improved significantly when prepared outside the glovebox due to sonication just before deposition, unlike those processed inside the glovebox even with methyl functionalized BaTiO<sub>3</sub> NPs (Fig. 9).

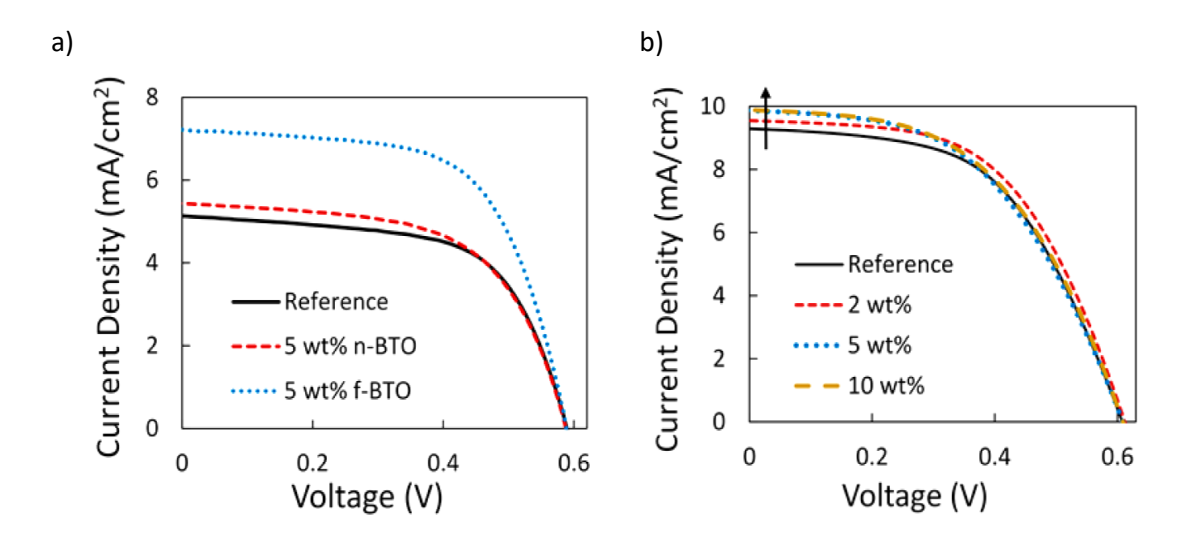


Fig. 9. J-V curves for OPV devices prepared in air (a) and inside the glovebox (b), n-BTO refers to neat BaTiO3 while f-BaTiO₃ stands for methyl-functionalized BaTiO₃ NPs [43, 96].

# 3.2.2. Enhanced light absorption

The short diffusion length ( $L_D$ ) of excitons is one of the main limitations of OPVs, which sets an upper limit to the thickness of the active layer. Therefore, light absorption by the device is restricted to the thickness of the active layer. In contrast, if the active layer is too thick, the majority of excitons will recombine before dissociation into free carriers. A compromise must thus be reached for maximum light harvest and reduced recombination. A promising approach to increase the absorption by the active layer without increasing its thickness can be achieved by increasing the path length of the incident photons within the photoactive layer through scattering, which increases the interaction time between photons and the absorber. Light scattering within the active layer was also realized by doping the active layer with relatively large metal oxide NPs. In addition, slight enhancement in light harvest due to scattering, resulting from the different refractive indices between the D/A blend and NPs, has been reported for wide bandgap NPs with average size of 50 nm [43, 96]. However, the light scattering by such NPs was found to increase with increasing the refractive index contrast.

Metal oxide NPs offer further advantages over MNPs such as their wide bandgap energy, which make energy losses negligible when added to the active material of OPVs. In addition, the low cost of metal oxide NPs makes them a good choice for improving the device performance. Easily fabricated and cost-effective SiO<sub>2</sub> NPs with an average size of 160 nm were incorporated into PEDOT: PSS HTL of

a P3HT:  $PC_{61}BM$ -based solar cell. The modified device showed a ~17.5% increase in  $J_{SC}$  and a ~7% in PCE due to the enhanced scattering by dopant NPs and hence increased path length of light photons within the photoactive layer [97] as shown in Fig. 10.

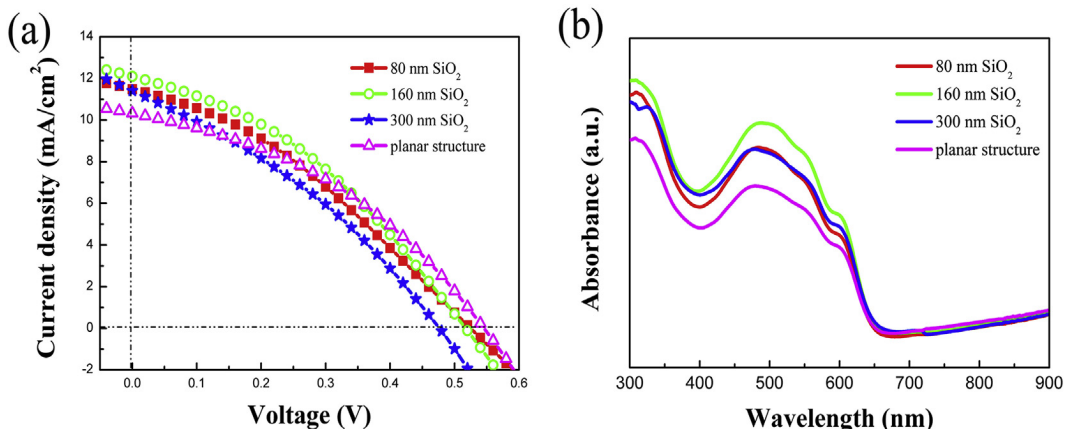


Fig. 10. (a) Illuminated J-V curves at AM 1.5G and (b) light absorption of the samples after embedding SiO₂ nanoparticles with the diameter of 80, 160 and 300 nm. The corresponding data from the planer reference sample without SiO₂ nanoparticle embedding are presented for comparison [97].

# 3.3. Semiconducting NPs

Inorganic semiconductor NPs have shown significant potential to enhance the efficiency of organic solar cells through multiple pathways. The remarkable features of semiconductor INPs such as their low cost, tunable absorption, high stability, and excellent electron mobility make them excellent candidates not only as nano-dopants to OPVs but also as electron acceptors in organic-inorganic hybrid solar cells [54, 98-100]. More details on the application of different inorganic semiconductor nanostructures on hybrid solar cells can be found in a comparative review by Wright and Uddin.[54] The bandgap of semiconductor INPs vary significantly from that of the bulk material due to quantum confinement effect [100-102] and can be controlled by changing their physical dimensions according to Eq. (8) [103]:

$$E_{g, confined} = E_{g, bulk} + \frac{\pi^2 \hbar^2}{2\mu R^2} - 1.786 \frac{e^2}{4\pi \varepsilon_0 \varepsilon_r R^2}$$
(8)

Where  $\mu$  and R represent the electron-hole reduced mass and the particle radius, respectively.

Thus, the optical absorption of semiconductor INPs can be tuned to be complementary to that of the active layer. In addition, light scattering induced by the presence of semiconductor INPs within the layers of an OPV device increases the path length of the incident sunlight and as a result, light harvest increases. The addition of semiconductor INPs into the photoactive layer of the device can also enhance the transport properties of OPVs through morphology optimization and carrier extraction and blocking effects supported by the electronic structure of such NPs [47, 104] as discussed below.

#### 3.3.1 Enhanced morphology

According to Eq. (1), the enhancement of any of the processes included in the photovoltaic effect in organic solar cells will increase the EQE and PCE of the device. After light is absorbed by the active layer, the photo-generated excitons diffuse within the donor over a short distance ( $L_D$ ) for a short time, exciton lifetime ( $\tau$ ), before recombination. Thus, excitons must be separated into free electrons and holes before recombination. The separation of excitons occurs at the donor-acceptor D/A interface if sufficient driving force is provided. The distance between the neighboring D/A interfaces should be

minimum for efficient diffusion and dissociation of excitons. Therefore, the morphology of the photoactive layer crucially affects the overall performance of the fabricated device. The formation of nano-scale interpenetrating networks between the electron-donating and electron-accepting materials enhances the diffusion of excitons and reduces their recombination rate [105].

Once the dissociation of excitons happens at the D/A interface, the free charge carriers are transported within the active layer to the respective electrodes. Free electrons move through the acceptor towards the cathode, while free holes move to the anode within the donor. The efficient transport of carriers depends on the ability of electrons and holes to move easily through the acceptor and the donor, respectively. Thus, high mobility of holes ( $\mu_h$ ) and electrons ( $\mu_e$ ) are necessary for high photovoltaic performance, see Eq. (6). In addition, the balance between the mobility of electrons and holes ( $\mu_h/\mu_e$ ) increases  $J_{SC}$  and PCE of the device [106, 107]. The morphology and crystallinity of the photoactive layer likewise affect the mobility of free charge carriers and the overall efficiency of OSCs [34]. For solution processing methods, the selection of solvents as well as post treatment greatly influence the morphology of the photoactive layer [28, 29].

The utilization of semiconductor NPs in OPVs was found to improve the charge transport properties of the active layer due to improving the morphology, crystallinity and carrier mobility [45]. In this context, semiconducting NPs such as CuO (<50 nm), Cr<sub>2</sub>O<sub>3</sub> (23 <d< 34 nm) and ZnO (<100 nm) nano-dopants showed great potential to improve the optical absorption, morphology, and device efficiency [45-47]. For instance, CuO NPs were used as a third component in a ternary OPV device. The PCE of the device has increased from 3% to 4.1% as a result of enhanced morphology and crystallinity, which improved the mobility of electrons and holes, light harvest (via scattering), charge transport and exciton dissociation. In contrast, the high doping concentration of CuO NPs had a negative impact on the device performance, as shown in Fig. 11, as a result of large agglomerations that act as recombination centres, as confirmed by SEM images (Fig. 12), and reflected on the values of carrier mobility and R<sub>SH</sub> [47]. Additionally, Liu et al. [45] investigated the impact of Cr<sub>2</sub>O<sub>3</sub> NPs doping on the active layer of P3HT: PCBM and PCDTBT: PC70BM based devices. With respect to their control devices, the PCE of the doped device increased from 3.02% to 3.5% and from 4.47% to 5.49% for the P3HT and PCDTBT based devices, respectively. These enhanced performances were attributed to a combination of effects induced by the dopant Cr<sub>2</sub>O<sub>3</sub> NPs. Atomic force microscope (AFM) images revealed significant phase separation, with slight changes in the roughness of the active layer, which subsequently improved charge transport (see Fig.14).

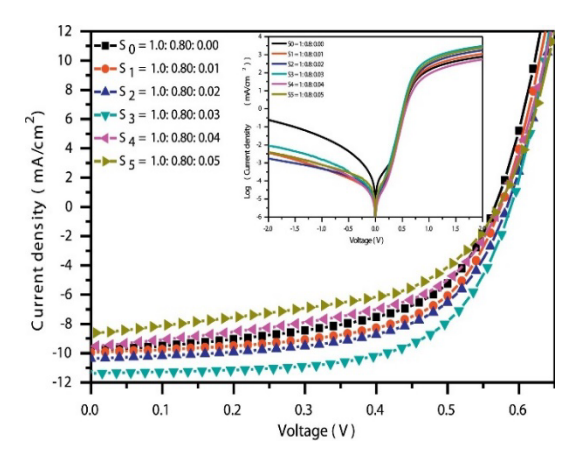


Fig. 11. J-V characteristics under AM 1.5 G standard light intensity of ITO/ZnO/P3HT: PCBM: CuO NPs/MoO3/Ag hybrid solar cells.[47]

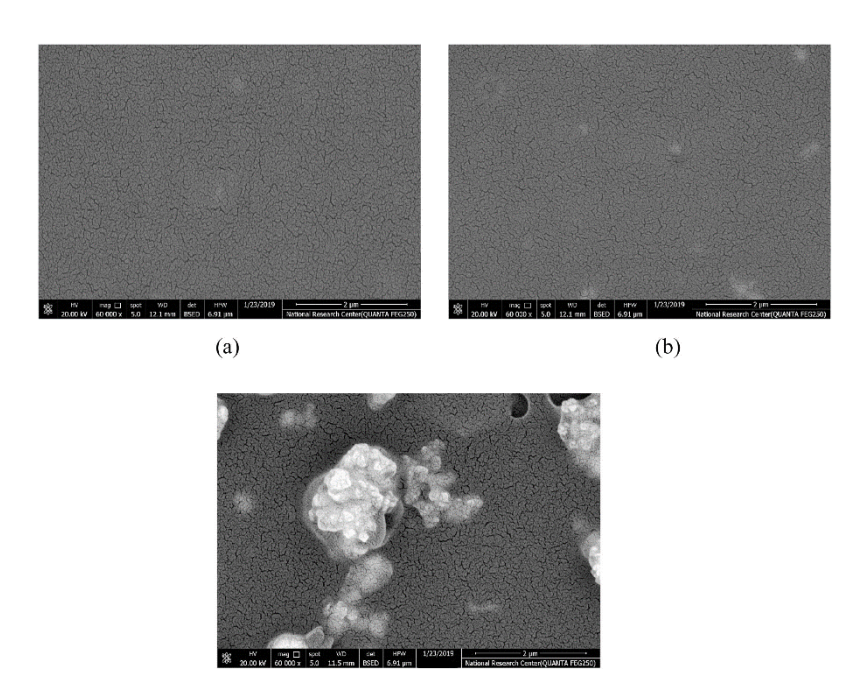


Fig. 12. SEM images of P3HT: PCBM: CuO NPs at ratios (a) 1:0.8:0.00, (b) 1:0.8:0.03 and (c) 1:0.8:0.05.[47]

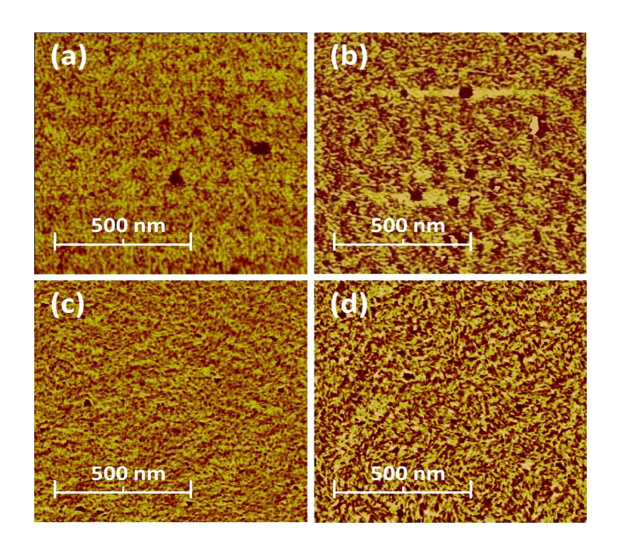


Fig. 13. AFM phase images of the P3HT/PC60BM surfaces (a) without and (b) with  $Cr_2O_3$  nanoparticles, and PCDTBT/PC70BM surfaces (c) without and (d) with  $Cr_2O_3$  nanoparticles [45].

TiO<sub>2</sub> NPs resulted in a ~125% increase in the PCE of the device when added to the P3HT: PCBM active blend. The presence of TiO<sub>2</sub> NPs within the photoactive layer enhanced the nanoscale phase separation, which facilitated charge transport and dissociation of excitons as a result of the increased area of the D/A interface as depicted in AFM images (Fig 15A). In addition, the increased surface roughness of the doped active layer was proposed to reduce charge transport distance. Moreover, the light harvest of the doped device greatly increased compared to the control device due to absorption and scattering by the NPs. The outstanding improvement in both optical and transport properties of the TiO<sub>2</sub>-doped device was confirmed by photoluminescence (PL) and quantum efficiency measurements (see Fig. 14B and C). The device with an optimum ratio (20 wt%) TiO<sub>2</sub> exhibited the highest quenching in PL and highest IPCE over the investigated wavelength range.

Aggregations of the dopant NPs at high loadings increases carrier recombination and hence leads to a drop in device performance [104]. The application of semiconductor NPs to OPVs is not limited to the active layer, but can be expanded to buffer layers. Recently, NiS NPs were utilized as dopant in HTL resulting in ~95% improvement in PCE as result of their superior hole transport properties (Fig. 15a). The addition of 0.1% NiS NPs to the HTL resulted in a significant enhancement in the carrier mobility by approximately two orders of magnitude, which reduced carrier recombination as confirmed by space charge limited current (SCLC) measurements (Fig. 15b). The enhanced transport properties were attributed to the creation of extra and alternative pathways to the anode [108].

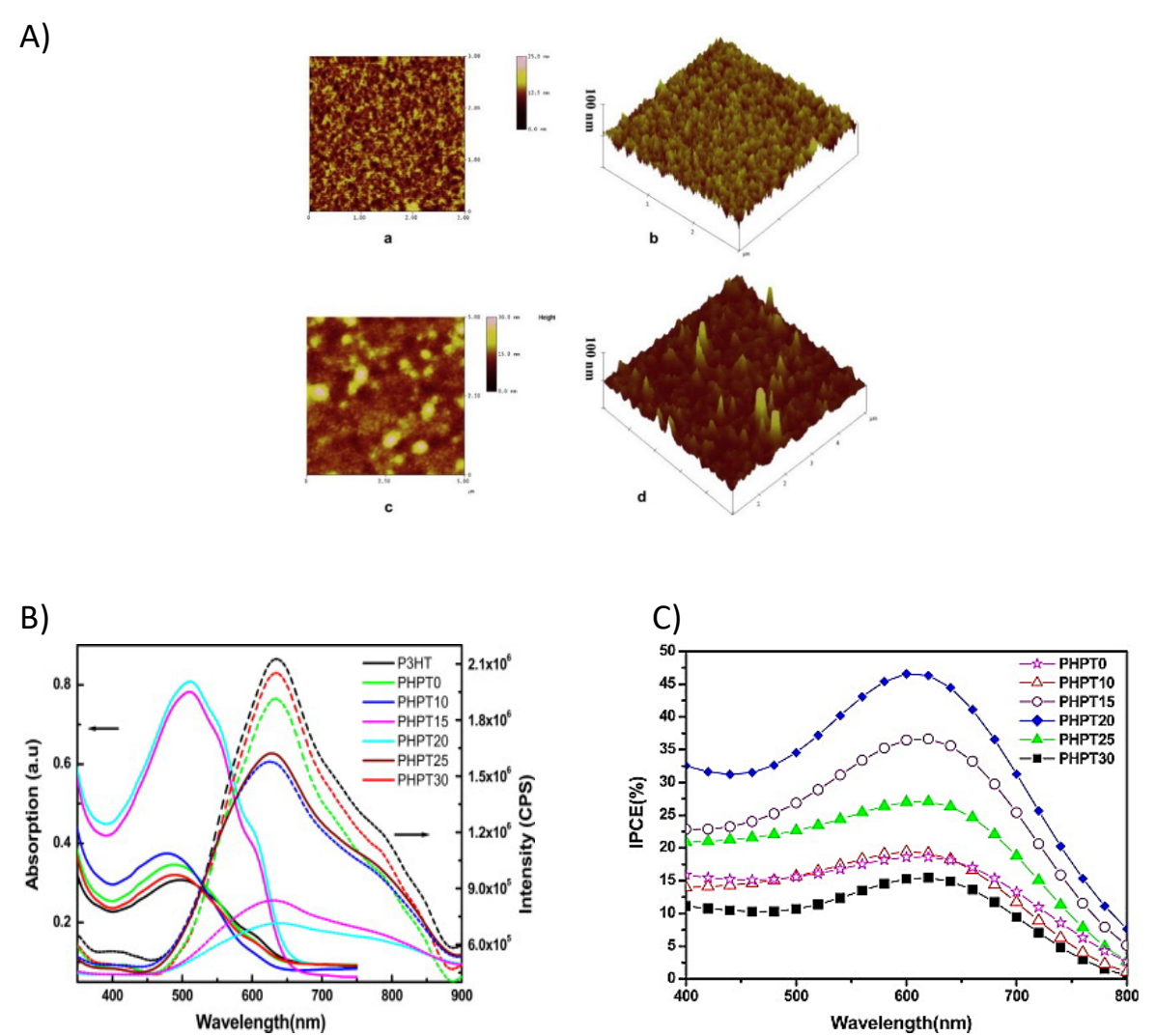


Fig. 14. (A) AFM images of the active layer films of the photovoltaic cells made with(a)(b) P3HT:PCBM and(c)(d) hybrid P3HT:PCBM:TiO2. (B) UV-vis absorption and PL spectra of pristine (P3HT:PCBM) and hybrid (P3HT:PCBM:TiO2) thin films. (C) Incident photon-to-current conversion efficiency (IPCE) curves for the pristine P3HT:PCBM and hybrid P3HT:PCBM:TiO2 photovoltaic cells. PHPT refers to P3HT: PCBM (1:1) with different wt% of TiO<sub>2</sub> [104].

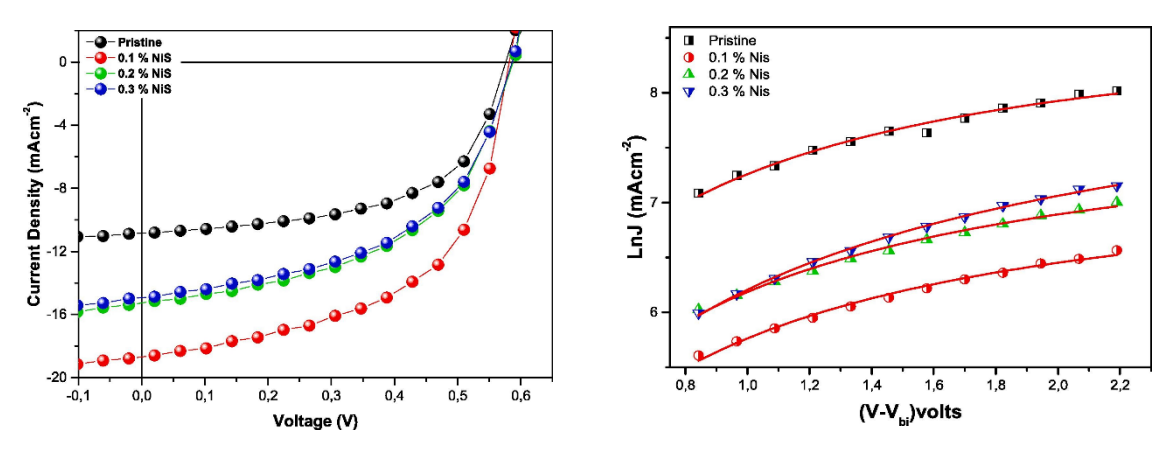


Fig. 15. (a) J-V characteristics of the best performing devices. (b) dots (..) represent the space charge limited currents of the diodes with solid lines representing computer fits [108].

#### 3.3.2. Improved carrier hoping

The incorporation of semiconductor NPs into the active layer can also enhance carrier hoping. This effect depends on the electronic structure and the relative position of the energy levels of the dopant NPs with respect to those of the donor, acceptor, and the electrodes. If the edge of the conduction band ( $E_c$ ) of the dopant semiconductor NPs lies between the LUMO level of the acceptor and the fermi-energy of the cathode, electron hoping is facilitated. Moreover, when the valence band edge ( $E_v$ ) of the dopant semiconducting NPs is lower than the HOMO of the donor, an energy barrier is formed which prevents hole-leakage from the donor. This blocking effect is similar to that offered by buffer layers used between the active layer and the electrodes of the device. In addition, semiconductor INPs within the active layer can also work as an electron acceptor ifa proper heterojunction between the semiconductor NPs and the donor can be formed (staggered band junction) [54, 104].

The improved carrier extraction by semiconductor INPs leads to an increased mobility of charge carriers. In addition, the carrier blocking effect results in the suppression of leakage currents, which is directly reflected on the shunt resistance of the device. The value of R<sub>sh</sub> can increase significantly when leakage current is reduced. In addition, the improved carrier extraction and transport through the active layer cause R<sub>s</sub> to decrease. Therefore, inorganic semiconductor nanodopants can improve J<sub>SC</sub>, V<sub>OC</sub>, and FF simultaneously, which consequently results in an outstanding increase in PCE of the device. The incorporation of TiO<sub>2</sub> NPs into a P3HT: PCBM blend has resulted in an enhancement of 42%, 36%, and 17% in Jsc, Voc, and FF, respectively, which as a result increased the PCE of the device from 1.5% to 3.36% [104]. The enhanced photo-generation and the reduced recombination was confirmed by EQE and PL data (Fig. 13). Similarly, the addition of Cr₂O₃ NPs to the P3HT: PCBM has enhanced  $\mu_e$  of the device due to facilitated electron hoping mediated by the  $E_c$  of Cr<sub>2</sub>O<sub>3</sub>. The increased shunt resistance and FF was assigned to the reduced hole leakage current due to the low E<sub>V</sub> of Cr<sub>2</sub>O<sub>3</sub> and subsequent blocking effect as discussed above [45]. The PCE enhancement achieved with TiO2 (125%) is much higher than that with Cr2O3 (18% and 22%), which may be attributed to the highly increased optical absorption (in case of TiO<sub>2</sub>) as a result of the increased surface roughness, which enhanced internal scattering of light. In addition, the lower E<sub>c</sub> level (4.2 eV) of TiO<sub>2</sub> compared to that of Cr<sub>2</sub>O<sub>3</sub> (3.93 eV) might lead to better extraction of electrons.

The effect of different semiconducting nanostructures on the performance of OPVs was also reported by other research groups [109-112]. For instance, Lu and co-workers reported that Cu₂S nanodisks can improve the photovoltaic performance of P3HT: PCBM-based OSCs when used as

dopant to the active layer. An increase of 22.7% in PCE of the device with optimum doping compared to that of the reference device was achieved. This behaviour was explained by the improved electron mobility of the active blend, which facilitated the transport of charges [113]. An increase in PCE of up to 10% was realized by the incorporation of CdS NPs into the active blend of PTB7: PCBM, which was caused by an enhanced morphology that facilitated charge transport and dissociation of excitons [114]. A major application of semiconductor INPs is as ETL or HTL depending on the position of  $E_v$  and  $E_c$  with respect to the HOMO and LUMO of the donor and acceptor materials and the fermi level of the electrodes. For instance, ZnO NPs have revealed promising potential as ETL in an inverted geometry OPVs [115, 116].

#### 3.4. Magnetic NPs

#### 3.4.1. Intersystem crossing

The short diffusion length ( $L_D$ ) and lifetime ( $\tau$ ) of excitons are major limitations of organic solar cells due to high recombination losses [117]. The photo-generated excitons within the active layer can exist in either a singlet or triplet state with extremely variant lifetimes and hence diffusion lengths [118]. In a singlet excited state, the electron spin is anti-parallel to the ground state electron, while for triplet state, the electron spins parallel to the ground state electron (Fig. 16). According to the Pauli Exclusion Principle, electrons occupying the same energy state must have antiparallel spin. Thus, when a photon is absorbed by an electron in the ground state, it is more probable to form a singlet excited state than triplet excited state as the later requires spin conversion of the excited electron. Singlet  $\rightarrow$  singlet transition is much easier than singlet  $\rightarrow$  triplet or triplet  $\rightarrow$  singlet transitions. Therefore, the number of singlet excitons forming in the active layer by light absorption is much higher than that of their triplet counterparts. Triplet excitons have much longer lifetimes and diffusion lengths than singlet counterparts [119].

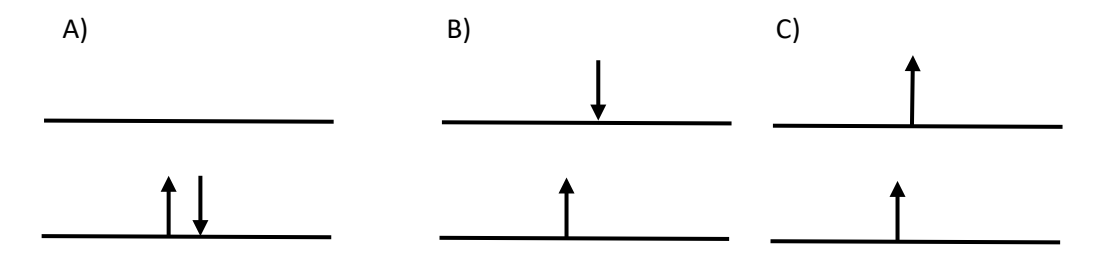


Fig. 16. Schematic diagram for singlet ground state (A), singlet (B) and triplet excited (C) states

Singlet-state excitons generated in P3HT have shown lifetimes in the range of 300 ps and  $L_D$  up to 6 nm, [120, 121] while triplet excitons exhibited much longer  $\tau$  (10  $\mu$ s) leading to larger  $L_D$  reaching 100 nm [122]. Thus, increasing the population of triplet excitons within the photoactive layer is expected to increase the PCE of the device due to improved transport properties and suppressed recombination of excitons [123-125]. Thus, if the conversion from singlet to triplet excitons can be accomplished, higher photovoltaic efficiency can be realized. It was found that the interaction of a weak magnetic field with excitons can increase their lifetimes and diffusion lengths [126, 127] based on the intersystem crossing (ISC) process in which singlet excitons are converted into triplet states.

The interaction between ferromagnetic NPs with moving charges such as excitons within the active layer of an organic solar cell can induce a weak magnetic field within the active layer.[44] Therefore, the incorporation of magnetic NPs into the active layer of OPVs was realized by many

research groups as an effective strategy to improve the PCE of the device through intersystem crossing [128-131]. In this context, Zhang *et al.* were the first to incorporate the super ferromagnetic  $Fe_3O_4$  NPs capped with oleic acid (OA) within the active layer of an OPV device leading to about 18% increase in PCE compared to the non-doped counterpart. The enhancement in PCE of the device with optimum OA- $Fe_3O_4$  (Fig. 17) doping concentration was mainly due to the increase in  $J_{SC}$ , which was attributed to the increased population of the long-lived triplet excitons [128].

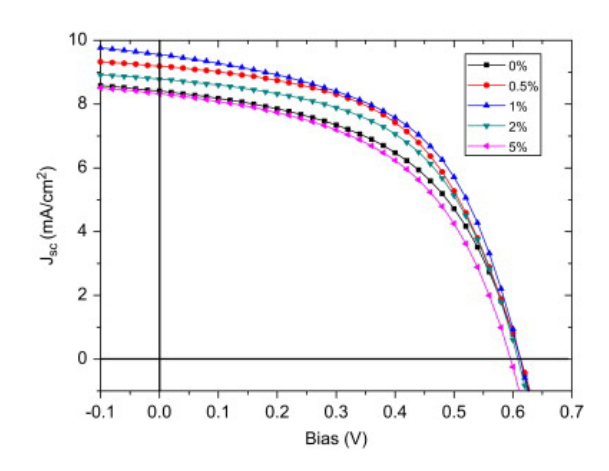


Fig. 17. J-V curves of P3HT:PCBM BHJ-PSC with and without OA-Fe3O4 NPs [128].

#### 3.4.2. Coercive electric field

It is worthy to mention that approximately 50% of the efficiency losses by OPVs are caused by carrier recombination as a result of the low  $\varepsilon$  of organic semiconductors as well as morphology imperfection [15, 16]. The photo-generated excitons exhibit two competitive effects: sweep-out by internal electric field and carrier recombination pathways either geminate or non-geminate [132]. The efficient collection of the photo-generated charge carriers in an OPV device requires an electric field intensity in the range of 50-70 V/ $\mu$ m under reverse bias and short-circuit conditions [56, 57]. The built-in electric field ( $E_{bi}$ ) arising from the energy offset between the work functions of the electrodes is insufficient for collecting all the generated carriers. For instance, if the difference between the work function of both electrodes is <2 eV and assuming device thickness of only 100 nm, then an electric field of 20 V/ $\mu$ m results. Thus, this electric field is unable to suppress the recombination of the majority of the generated charge carriers [57, 121].

Consequently, strengthening the electric field through the device should lead to effective carrier collection and hence improved PCE of the device. In addition to ISC effect, the incorporation of ferromagnetic NPs, with their magnetic dipoles aligned, in the photoactive layer was found to be an efficient strategy to strengthen the electric filed within an organic solar cell. The alignment of the magnetic dipoles of the dopant NPs is achieved by the application of external magnetic field during device fabrication. The interaction between aligned magnetic dipoles results in a coercive electric field ( $E_C$ ) that increases the induced electric field leading to enhanced charge collection [133]. The value of the coercive electric field can be described as: [134, 135]

$$E_C = \frac{4\pi\sigma f}{\varepsilon} \tag{9}$$

Where,  $\sigma$  is the surface charge density, and f is the volume fraction of the dopant magnetic NPs.

The generation of  $E_C$  within the device improves the sweep-out and dissociation of excitons. Furthermore, a large  $\varepsilon$  of the magnetic NPs can help to increase the total electric permittivity of the doped active layer. It was reported that the addition of FeO<sub>3</sub> NPs with relative permittivity ( $\varepsilon_r$  = 20) to P3HT: PCBM film ( $\varepsilon_r$  = 4) can result in 25% increase in the permittivity of the composite, [136] which subsequently improves exciton dissociation. More importantly,  $E_C$  increases the drift velocity and kinetic energy (K.E) of the electrons and holes. Therefore, the reduced attraction force between the electron-hole pair as well as their increased (K.E) cause the total energy (U) of excitons to increase as: [137]

$$U = \left| E_{Donor}^{DHOMO} - E_{Acceptor}^{LUMO} \right| - E_B + \frac{1}{2} m_e^* V_e^2 + \frac{1}{2} m_h^* V_h^2$$
 (10)

Where  $m_e^*$  and  $m_h^*$  stands for the effective mass of the LUMO electron and the HOMO hole respectively.

As a result of the increased U of the exciton, it becomes unstable and tends to dissociate into free carriers. In this context, Wang et al. [137] incorporated  $Fe_3O_4$  into the photoactive layer of OPVs while applying an external magnetostatic field during deposition of the doped active layer for further orientation of the magnetic dipoles inside the BHJ D/A layer. This strategy improved the cell performance via different mechanisms such as strengthening of the electric field through the device, as discussed above. In addition, the mobility of charge carriers as well as the morphology of the active layer improved significantly. Furthermore, the high dielectric constant of  $Fe_3O_4$  NPs facilitated exciton dissociation. The results shown in Fig. 18 reveal that the PCE of the devices with  $Fe_3O_4$  NPs increased by 28% without and 50% with the application of the external magnetic field, respectively. The application of an external vertical magnetostatic field on the  $Fe_3O_4$ -doped active layer during the spin coating of the active layer rearranged the magnetic dipoles within the NPs inside the active layer (Fig. 19). The charge distribution on the surface of the aligned dipoles (NPs) induces a coercive electric field within the active layer, which greatly enhances charge transport through the device for efficient collection at the respective electrodes.

It can be observed from Fig. 18 that the doped device without the application of an external magnetic field showed a poorer improvement than the devices with an external field applied. The arrangement of the dipoles by the external magnetostatic field not only lead to the generation of E<sub>C</sub>, which facilitates exciton dissociation, but also improved film morphology. The enhanced morphology resulted in better transport of the free charge carriers and hence an efficient collection at the respective electrodes as confirmed by the increased J<sub>SC</sub> and EQE.

More results on different magnetic NPs can be found in ref. [128-131], where aligned and non-aligned superparamagnetic ( $ZnFe_2O_4$  &  $NiFe_2O_4$ ) and ferromagnetic ( $CoFe_2O_4$ ) NPs doped small molecule OSCs. For example, the impact of  $ZnFe_2O_4$ ,  $NiFe_2O_4$ , and  $CoFe_2O_4$  NPs on the performance of the device with an active layer of DPP(TBFu)2: T60BM was investigated [131]. Except for  $CoFe_2O_4$  based devices, all other devices experienced improvement in their PCEs with respect to the reference device. The degradation of the  $CoFe_2O_4$  device's performance was attributed to the aggregation of the dopant NPs as a result of their remnant magnetization. Furthermore, the large crystal size of  $CoFe_2O_4$  and the aggregation effect resulted in alternative pathways to the generated charge as confirmed by the reduced  $R_{sh}$  despite the dropped  $R_s$ . Noteworthy, the performance enhancement in case of the doped polymer solar cell in ref. [137] is higher than that in case of the doped OPVs in ref. [128-131]. This difference may be attributed to the different preparation methods, especially for the alignment

step, which was carried out during the spin coating of the polymer-based device, but was done after the deposition of the top electrode in ref. [128-131].

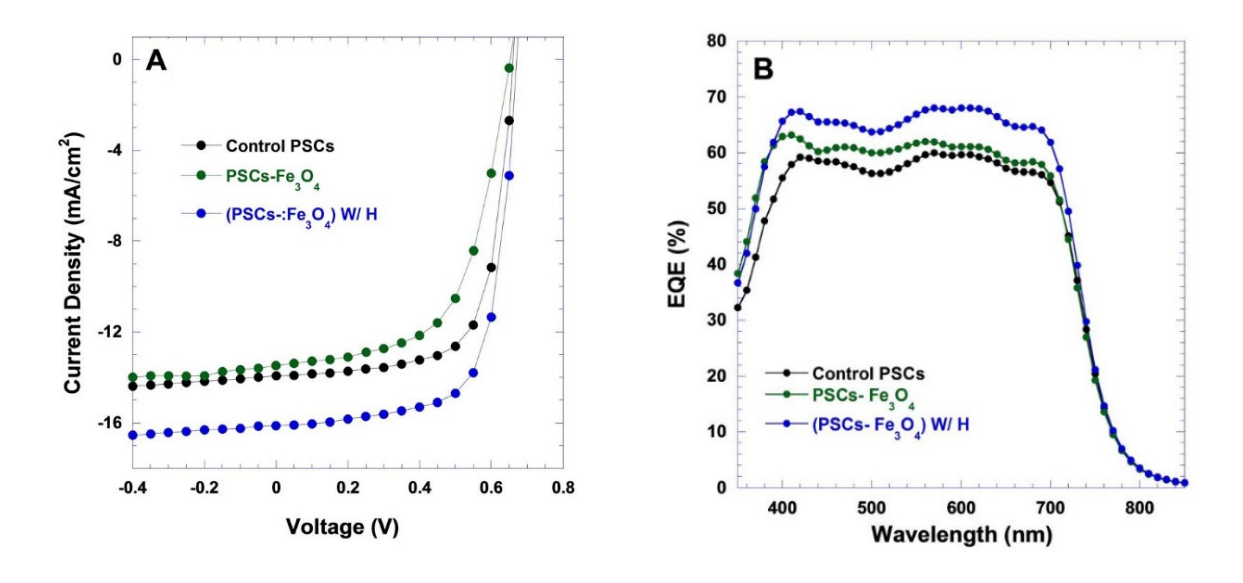


Fig. 18. (A) J–V characteristics of PSCs measured under 100 mW/cm<sup>2</sup> AM 1.5 G illumination, and (B) IPCE spectra of BHJ PSCs versus wavelength [137].

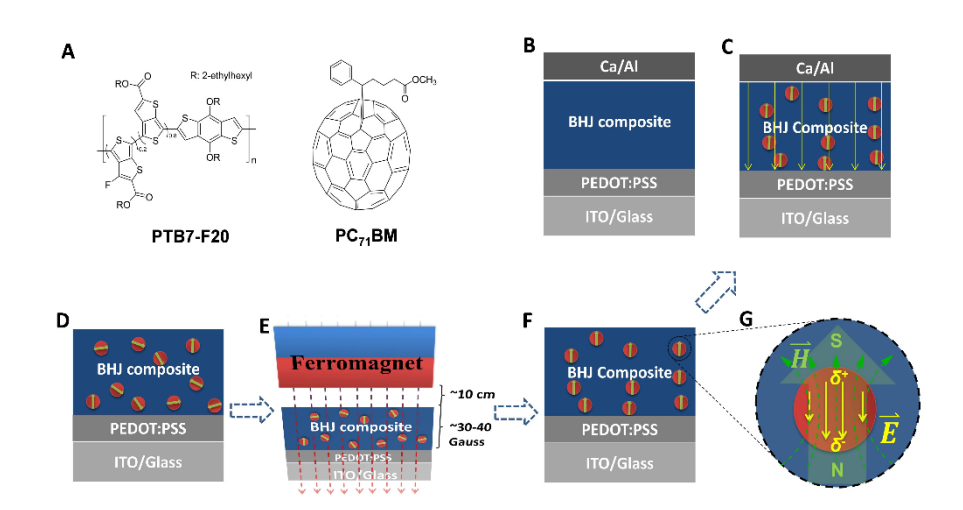


Fig. 19. (A) The molecular structures of PTB7-F20 and PC71BM; (B) the conventional device structure of PSCs without incorporating any  $Fe_3O_4$  magnetic nanoparticels (MNPs); (C) the conventional device structure of PSCs incorporated with  $Fe_3O_4$  MNPs and aligned by an external magnetostatic field; (D)–(F) the fabrication procedures of PSCs incorporated with  $Fe_3O_4$  MNPs and aligned by an external magnetostatic field; (D) BHJ active layer incorporated with  $Fe_3O_4$  MNPs was spin-coated on PEDOT:PSS coated ITO substrate; (E) a ferromagnet was suspend above the surface of BHJ composite incorporated with  $Fe_3O_4$  MNPs layer. The magnetic intensity is,30–40 Gand the distance between the ferromagnet and BHJ composite layer is,10 cm; (F) oriented  $Fe_3O_4$  MNPs inside BHJ active layer by an external magnetostatic field. In pre-devices; (G) Drawing of partial enlargement of  $Fe_3O_4$  MNP in (C), showing an antiparallel relation between the magnetic dipole (caused by the  $Fe_3O_4$  crystal inside the particle) and electric dipole (caused by the difference of charge density between the inside  $Fe_3O_4$  and outside organic coater) [137].

## 3.5. Rare-Earth elements NPs

The conversion efficiency of a solar cell mainly depends on its ability to convert as much incident sunlight as possible into electricity. For any atomic or molecular system, the bandgap energy

 $(E_g)$  of the material determines the energy of the light it can absorb. An incident photon should possess enough amount of energy  $\ge E_g$  to excite an electron from its ground state to a higher energy state, and hence be absorbed. Photons with lower energies than  $E_g$  will simply be transmitted through the material. On the other hand, photons with much higher energy than  $E_g$  will result in energy losses, mainly heat [17, 138].

The solar spectrum received by the Earth's surface consists of a higher portion of infra-red (IR) radiation (52%) and visible light (43%), with the remaining 5% within the ultraviolet (UV) region [18]. So far, the majority of donor polymers in OPVs can absorb within the visible region of the solar spectrum. Thus, PCEs of PVs in general and OPVs in particular are limited by this spectral mismatch. Therefore, the adjustment of the incident wavelengths by the solar cell via up- and down-converters has emerged as a promising strategy to enhance the light harvest by different categories of solar cells. Rare-Earth elements NPs have been utilized for the conversion of light for PVs. In the following, the physics and types of up- and down-converters as well as selected important findings related to their implementation in OPV systems will be discussed.

# 3.5.1. Up conversion nanoparticles (UC NPs)

The up-conversion (UC) process is based on the transformation of two or more low energy photons into a higher energy photon. This can be achieved by different systems such as rare-earth-doped up-conversion (RED UC) materials, triplet-triplet annihilation and up-conversion in quantum structures. However, RED UCs have been the most commonly used for PV applications due to their higher conversion efficiency compared to other approaches [139]. The rare earth elements consist of 15 lanthanide elements from lanthanum to lutetium ( $^{57}$ La –  $^{71}$ Lu) in addition to scandium ( $^{21}$ Sc) and yttrium ( $^{39}$ Y). The electronic structure of those elements enables them to absorb photons within the near infra-red (NIR) portion of the solar spectrum and remitting light quanta with shorter wavelengths, mainly within the visible region.[140-142] Light up-conversion by RE materials can be achieved through different mechanisms such as excited state absorption (ESA), energy transfer up-conversion (ETU), photon avalanche (PA), and energy migration-mediated up-conversion (EMMU) [139].

Excited state absorption (ESA) occurs through the successive absorption of two low-energy photons to excite the atom from the ground state to the first excited state and then to the second excited state before relaxation to the ground state (Fig. 20a). The energy of the emitted photon is equal to the difference between the final state and the ground state, thus up-converting the energy of the incident photons [143]. For energy transfer up-conversion (ETU), two ions are required where one acts as a sensitizer and the other as an activator. An incident photon with long wavelength excites the sensitizer to the first excited state where the excited electron can transfer its energy to an electron within the activator that was already excited by another pump photon. Eventually, radiative decay for the excited electron to the ground state of the activator occurs leading to the emission of a photon with shorter wavelength than the pump photon (Fig. 20b).

ETU plays a crucial role in understanding the up-conversion luminescence in UP NPs as the majority of such NPs are doped with pairs of ions (sensitizer and activator) such as Yb<sup>+3</sup>/Er<sup>+3</sup>, Yb<sup>+3</sup>/Ho<sup>+3</sup> or Yb<sup>+3</sup>/Tm<sup>+3</sup>.[139, 144-146] However, ETU has been observed with single lanthanide ion-containing UC NPs such as Er<sup>+3</sup>-doped LiYF<sub>4</sub>[147] and Ho<sup>+3</sup>-doped NaGdF<sub>4</sub> [148]. ETU can also include other mechanisms such as successive energy transfers (SET) and cross relaxation (CR) UC, as shown in Fig. 20(b). For SET process (Fig. 20c) the sensitizer ion is excited by a pump photon from the ground state (E<sub>0</sub>) into its E<sub>1</sub>, then its energy is transferred to promote the activator into its first excited state. After that the activator is excited to its radiative state (E<sub>2</sub>) through another ET process instead of ESA. Finally, the relaxation of the activator from E<sub>2</sub> to E<sub>0</sub> emits a photon with higher energy than the incident photon. In contrast, CR ET occurs for identical ions, where both ions are excited to their E1 by pump

photons, then Ion I (sensitizer) transfers its energy to raise the activator into its  $E_2$  before relaxing to  $E_0$  (Fig. 20d).

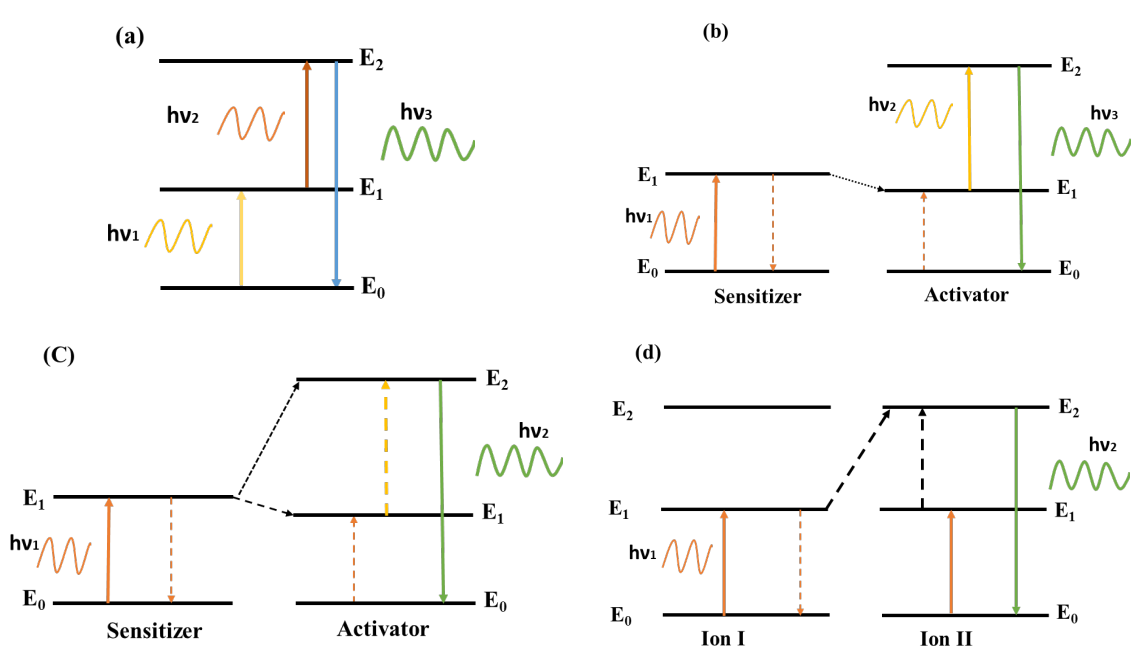


Fig. 20. (a) Excited state Absorption (ESA), (b) Energy transfer followed by ESA, (c) successive energy transfer (SET) and d) Cross relaxation up-conversion. Redrawn based on ref. [139] and ref. [149].

The third mechanism, as depicted in Fig. 21(a), of photon up-conversion with rare earth doped upconverters is known as photon avalanche (PA). In the PA, an incident pump photon is absorbed by an ion (I) that has been initially excited to its first excited state ( $E_1$ ). The pump photon subsequently populates the ion (I) to its second excited state (E2). Then, the increased population of E2 results in cross relaxation between the ion (I) and one of its neighbor ions (II) and hence raising both ions to their metastable state  $(E_1)$ . At this stage, two ions are in  $E_1$ , then with the next pump photon absorbed in the same way, four ions populate their E1, then eight and so on. The repetition of this process finally leads to an avalanche of ions populated in their E1 which, in turn, will be excited to E2 through the absorption of pump photons in an ESA process. Subsequently, the relaxation of these ions from their E2 to their ground states E0 produces upconverted photons with shorter wavelengths than the pump counterparts. It is important to mention that for PA to happen, the intensity of the incident light should exceed a particular threshold. If the excitation intensity is below this threshold, minor up-conversion can be observed, while at higher intensity than the threshold, UC increases significantly [149]. For the energy migration-mediated up-conversion to occur, it is essential to have four kinds of ions known as sensitizer, accumulator, migrator, and activator, respectively. Each ion plays a fundamental role in the up-conversion luminescence, starting when a ground state electron in the sensitizer ion is excited by an incident photon. Then, the excited electron transfers energy to the accumulator, which subsequently gives this excitation energy to the migrator ion. Eventually, the migrating energy is extracted by the activator, which in turn relaxes to its ground state emitting an upconverted photon as shown in Fig. 21(b) [143].

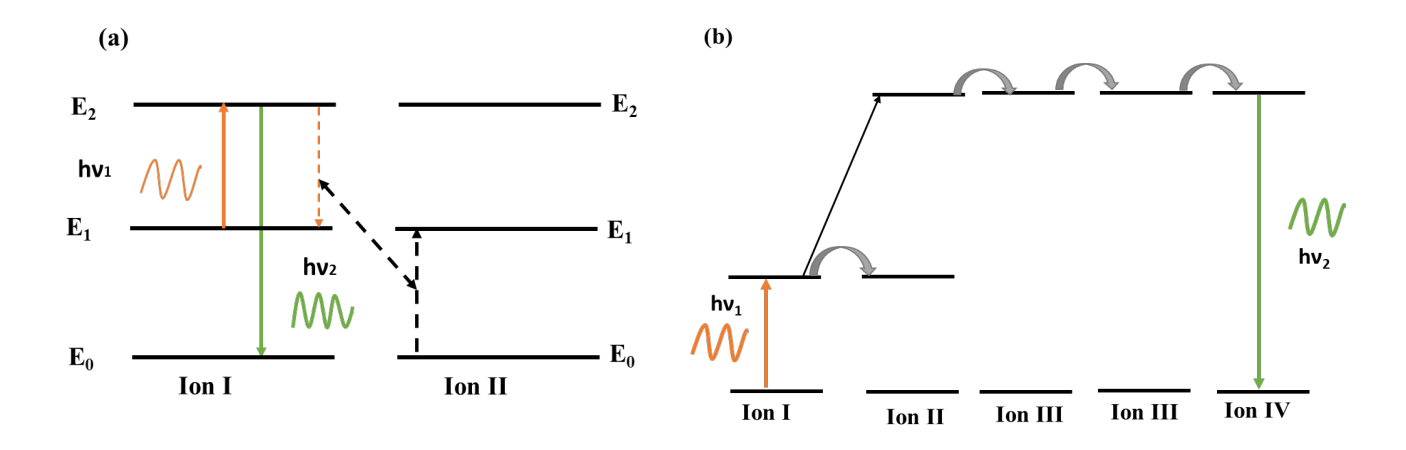


Fig. 21. Schematic representation of (a) Photon Avalanche and (b) Energy migration-mediated up-conversion.

Redrawn based on ref.[139]

#### 3.5.1.1. Structure of rare-earth doped upconverters (RED-UC)

RED-UCs consist of guest ion dopants, mainly trivalent lanthanide ions ( $Ln^{+3}$ ), in a dielectric host crystal such as a halide (fluorides, bromides, etc.). The host matrix not only houses the dopant ions, but also affects the whole process of light up-conversion. For efficient UC luminescence to occur, the host material should have a high transparency to low energy (NIR) photons, good thermal and chemical stability, structure matching with the  $Ln^{+3}$  ions, and low phonon energy. [150-152] Fluorides, phosphates and oxides have subsequently shown high potential as host substances for RED-UC NPs [153-156]. A fluoride based NaYF4 lattice was reported as one of the most efficient host materials for UC due to its low phonon energy, excellent optical and electric properties [157-159]. Generally, NaYF4 can exist in two phases, namely  $\alpha$  and  $\beta$ , describing cubic and hexagonal structures, respectively. It has been reported that the hexagonal structure is more efficient in terms of light upconversion due to its higher thermodynamic stability [160, 161].

The role of the dopant or guest ion is to absorb two or more pump photons that have a low energy and then re-emit a photon with higher energy. The guest dopant material can be a single ion (activator) or it can use an additional ion known as sensitizer, which improves the overall upconversion process. As discussed above, some UC mechanisms (ESA) occur within a single ion (activator), while others (e.g. PA) require the presence of a co-dopant (sensitizer). The sensitizer ion mainly excites the activator ion to a higher state through energy transfer to the activator. An efficient sensitizer should have a high absorption cross-section at the excitation wavelength as well as a resonance in its energy levels with the activator energy levels. These requirements are typically met by the ytterbium (70Yb) ion Yb+3 and hence, it was found to be the best sensitizer [162-164].

The application of UC NPs as dopants in the field of OPVs was first reported by Wang and coworkers in 2012 [165, 166]. MoO<sub>3</sub> layer doped with up-conversion nanocrystals based on Yb<sup>+3</sup>/Er<sup>+3</sup> was introduced as an efficient HTL in a regular geometry OPV device [165, 166]. The doped MoO<sub>3</sub> buffer layer had a dual functionality as a hole extraction layer as well as an up-converter system. Optical measurements revealed that the doped MoO<sub>3</sub> not only had a lower transmission (stronger absorption) than pristine MoO<sub>3</sub>, but also emission peaks that greatly matched the absorption wavelengths of the P3HT donor polymer (Fig. 22). The PCE of the Yb/Er doped device increased from 1.5% to 2.12% under 1 sun illumination because of the increased J<sub>SC</sub>, V<sub>OC</sub> and FF compared to the

reference device. The performance improvement cannot be attributed to the light up-conversion effect alone as V<sub>OC</sub> and FF improved as well. The doped HTL revealed enhanced electronic properties in addition to the light up-conversion effect. In the same context, Liu *et al.* have found that adding a trace amount of NaYF4: Yb<sup>+3</sup>: Tm<sup>+3</sup> NPs to TiO<sub>2</sub> ETL remarkably enhanced the efficiency of the device. The improved performance with the doped ETL, as shown in Fig. 22(b), was attributed to a triple-role played by the dopant NPs, leading to better optical and electrical properties compared to the pristine devices. Measurements showed that in addition to the conversion of NIR photons into visible light, the dopant NPs also increased photo-generation of excitons via light scattering. Moreover, series and shunt resistance measurements confirmed that devices with optimum dopant concentration showed better electron transport properties than their non-doped counterpart [167]. In addition, NaYF4: 2%Er<sup>+3</sup>: 18%Yb<sup>+3</sup> UC NPs were used to dope PEDOT: PSS HTL in both regular and inverted geometry OPVs. The results obtained confirmed that both light scattering and up-conversion caused improved device performance, with scattering having a stronger effect than photoluminescence of UC NPs [168].

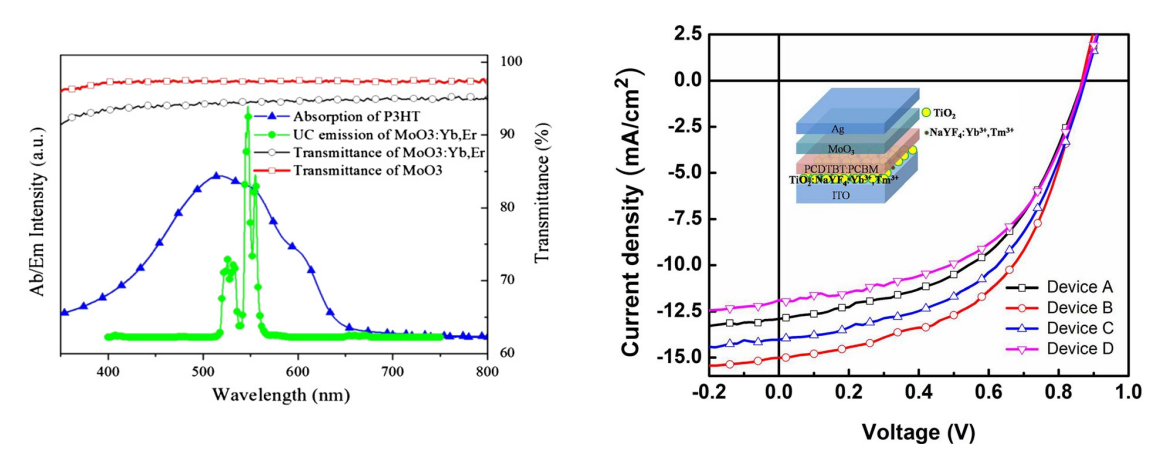


Fig. 22. (a)Optical properties of P3HT film, doped and un-doped MoO3 HTL.[165, 166] (b)The J-V characteristics of devices doping with different concentrations of NaYF4: Yb<sup>+3</sup>, Tm<sup>+3</sup> at 100 mW cm<sup>-2</sup>, inset is the device structure of inverted organic solar cell [167].

The addition of UC nanostructures to the photoactive layer was studied widely. For example, NaLuF<sub>4</sub>: Yb<sup>+3</sup>, Tm<sup>+3</sup> nanorods were used with PCDTPT: PC<sub>71</sub>BM-based OSCs, which resulted in a 19% improvement in PCE compared to the pristine device. The photovoltaic performance of the doped cells was enhanced as a result of scattering of the incident photons as well as conversion of IR into visible light [169]. Besides up-conversion of sub-bandgap photons, it was reported that NaYF<sub>4</sub> NPs can increase light harvest by the active layer through scattering [167, 170]. The dual function (up-conversion and scattering) of the dopant NaYF<sub>4</sub> NPs improved  $J_{SC}$  of the PCDTBT: PCBM-based inverted architecture OPV device and hence the PCE exhibited a nearly 19% increase with respect to the control device [170].

Early attempts utilized UC nano crystals (NCs) to enhance the performance of OPVs without disturbing the electrical properties of the device [171, 172]. UC systems were coated either in the front or rear side without being incorporated into different layers to avoid any possible suppression of the transfer of charge throughout the various layers of the device (Fig. 23). For instance, Wu  $et\ al.$  spray-coated a relatively thick film (5  $\mu$ m) of NaYF4: Yb/Er NCs on the backside of the glass substrate of a regular geometry OPV device with the structure ITO/ PEDOT: PSS/ P3HT: PCBM/Ca/AI [172]. The

device performance was found to improve when illuminated by a monochromatic (980 nm) laser beam with 146 mW compared to the reference device. This enhancement was attributed to an UC process, especially due to the overlap between the emission lines (~550 and 650 nm) of NaYF4/Yb/Er with the absorption of P3HT: PCBM, as well as the absorption of NIR photons by charge transfer states [173]. However, the photovoltaic parameters were found to decrease dramatically under soar simulator illumination (AM1.5G) (Fig. 24). This drop was assigned to the attenuation of the incident photons via scattering and absorption, hence reducing the light intensity that reaches the active layer. Moreover, UC is less effective when the intensity of excitation radiation is insufficient.

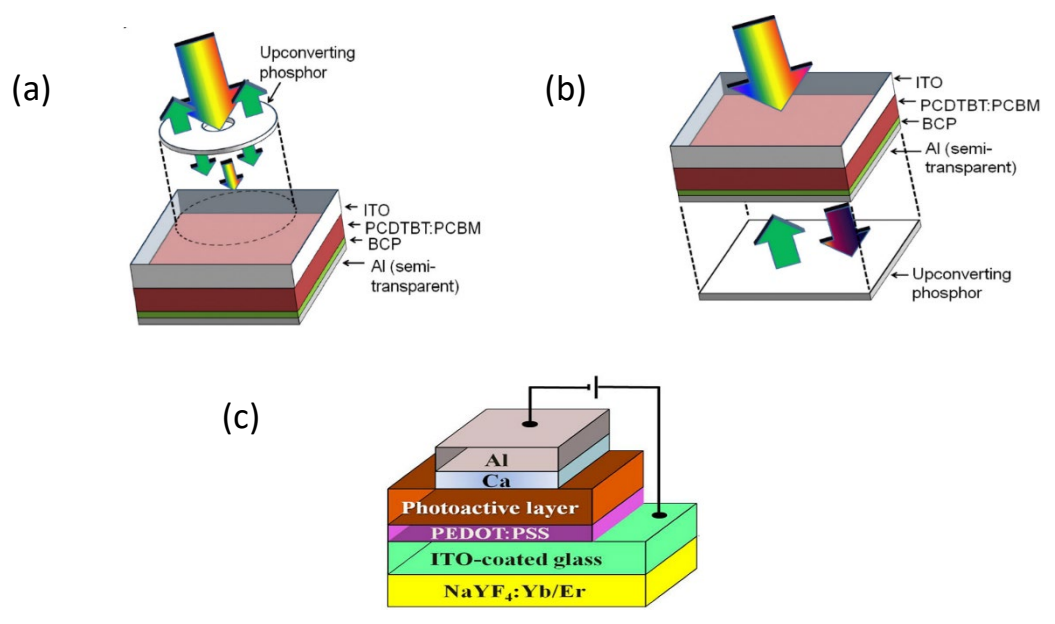


Fig. 23. Schematic of the organic photovoltaic device with an up-conversion phosphor placed in front (a) and behind the device (b). In (a) and (b) the separation of the phosphor from the device was ~ 0.5 mm [171]. (c) schematic representation of the structure of the OPV incorporating NaYF4:Yb/Er phosphors [172].

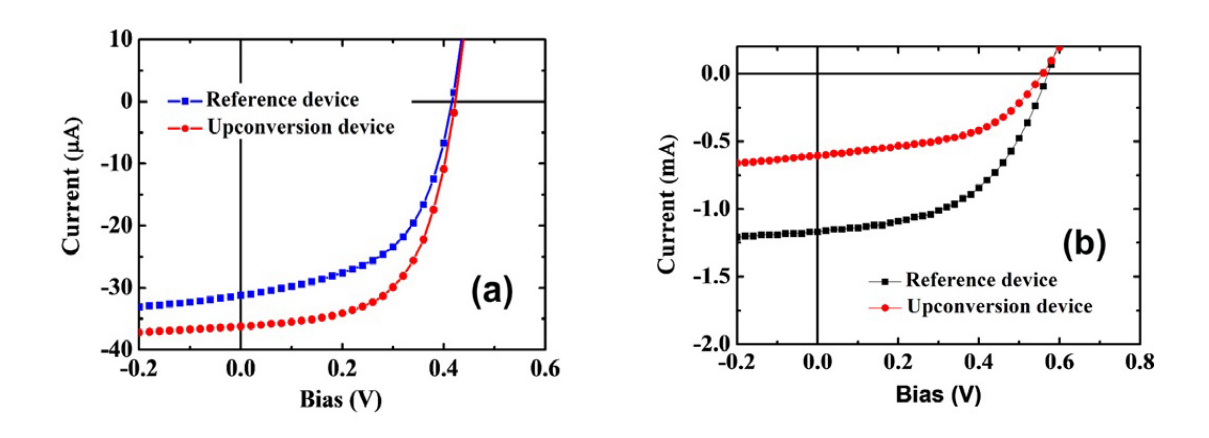


Fig. 24. I–V characteristics of OPV devices, recorded under illumination with (a) a 980-nm laser at a power of 146 mW and (b) simulated solar light (AM 1.5G) at 100 mWcm<sup>-2</sup> [172].

Thus, the application of UC NPs into OPVs can be divided into three approaches.

- 1. Incorporating UC NPs into the active blend: an improvement in the PCE of the device can be observed not only due to light up-conversion, but also scattering effects.
- 2. Addition of UC nano-dopants to the buffer layers, ETL or HTL: This method has shown a great potential to improve the device performance as it was found to positively affect optical absorption and charge transfer as well as light up-conversion properties.
- 3. Addition of UC-based structures to the front or the rear side of the device: Sub-bandgap photons (NIR and IR) are converted into visible light that can be absorbed by the donor: acceptor blend without interference with the different layers of the device and hence disturbance of charge transport through such layers can be avoided. Additionally, this approach helps to investigate the role of up-conversion mechanisms in improving device performance.

#### 3.5.2. Down conversion (DC) nanoparticles

As mentioned earlier, the spectral mismatch between the incident solar radiation and the optical absorption of the active layer of OPVs represent a major limitation to their PCEs. When the energy of the incident photon is much higher than the bandgap energy of the absorber material, such as for UV, it cannot be converted into electricity, but is lost as heat instead [17, 138]. Down conversion (DC) was proposed as a promising approach to make use of such portion of the solar spectrum in PV devices. DC is a process in which a high energy photon is converted into two or more photons with lower energies.

DC can occur within either a single- or two-ion system. In a single-ion downconverter that have three energy states, an energetic photon can excite the ion into its highest excited state. Then, two subsequent relaxation events to lower states emit two photons with lower energy than the incident photon.[174] For a two-ion system, one of the ions is in its excited state as a result of photon absorption, then this ion excites the second one via energy transfer. Finally, both ions reach their ground states through the emission of two low-energy photons (Fig. 25) [17, 138, 175].

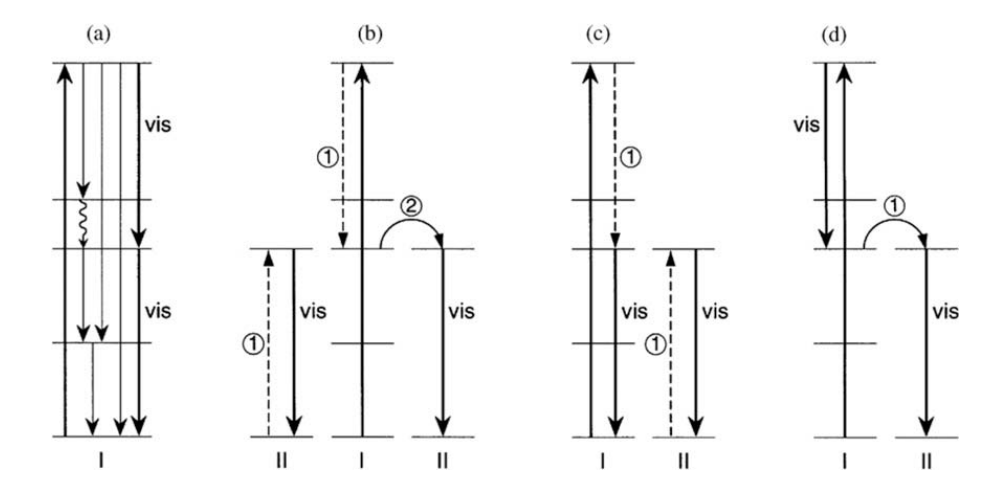
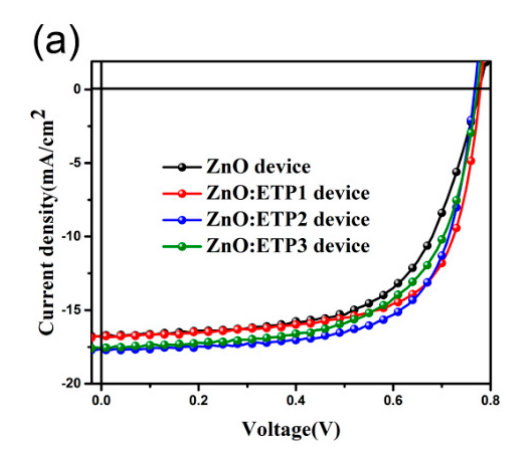


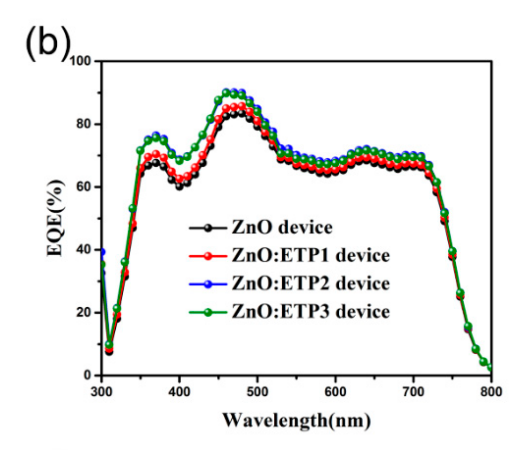
Fig. 25. Possible electronic transitions in a single ion (a) and two-ion systems (b, c, and d) ref. [17, 138, 175].

DC NPs were utilized in different types of solar cells including Si [176], dye-sensitized [177-179], hybrid and organic [180, 181] solar cells. Lanthanide ions as well as different nanostructures such as quantum dots [182], nanotubes [183], and nano-tips [184] are the main DC materials reported. Similar configurations to those used with upconverters were also employed with DCs. For OPVs, DC NPs were used as dopants to buffer layers such as reported by Svrcek *et al.* [180]. These authors added Si-nanocrystals to the PEDOT: PSS HTL in a conventional structure OPV device based on a PTB7:  $PC_{70}BM$  active layer. EQE measurements revealed an improvement in performance at short wavelengths (300-400 nm) for the doped device. However, the overall conversion efficiency dropped from 7.41% to 7.33% under 1 sun illumination. More interestingly, the efficiency of the doped device has enhanced under concentrated illumination <5 suns. Additionally, a bifunctional  $Eu^{+3}$  doped ZnO layer was reported as an efficient ETL that showed DC in the UV region without disturbing the electrical properties of the device [181].

Only small improvements in the PCE of OSCs were obtained through the addition of lanthanide DC ions to different layers of the device. This was attributed to the weak absorption as well as the limited amount of light harvested via direct excitation of the lanthanide ions, which can be addressed through the utilization of lanthanide organic complexes [185]. Organic ligands in such complexes have stronger absorption in the UV region than the lanthanide ions. In addition, organic ligands can efficiently transfer the absorbed energy to lanthanide ions, which in turn reemit those UV photons in the visible range through DC, hence increasing the amount of radiation harvested by the active layer of the device [186, 187]. Recently, Bu et al. have presented an efficient complex-DC material based on Eu<sup>+3</sup> ions and 1, 10 phenanthroline (phen) and 2-trifluoroacetonate (TTA) ligands- Eu (TTA)<sub>3</sub> phen (ETP). The new DC complex (ETP) was chemically added to the ZnO buffer layer, which resulted in a 13% improvement in the PCE compared to the control device. EQE data showed that the device with ETP downconverter had a higher absorption in the UV and visible range, which not only improved the device conversion efficiency but also increased the lifetime of the device as a result of effectively reducing the amount of UV reaching the active layer (Fig. 26) [188].

The improvement of OPV device performance achieved by UC and DC NPs as result of the wavelength conversion under sunlight illumination is still low. However, the easy processing as well as wavelength conversion range of RE NPs as UC and DC make them good candidates for improving the light absorption and the conversion efficiency of OPVs in the future. More research is still needed to improve the yield of UC and DC systems before their large-scale application in photovoltaics.





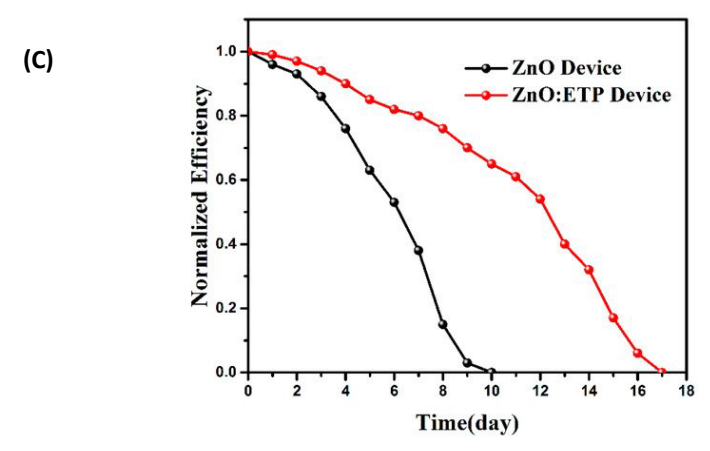


Fig. 26. (a) Current density versus voltage characteristics, (b) external quantum efficiency (EQE) curves of devices based on PTB7-Th–PC71BMusing ZnO and ZnO/ETP (different concentrations) as cathode buffer layers.(c) PCE decay curves of the ZnO and ZnO/ETP device (based on PTB7-Th–PC71BM) stored for 17 days in an N<sub>2</sub>-atmosphere [188].

# 4. Preparation methods of INPs-based OSCs

The fabrication of OSCs that implement INPs is based on almost the same procedure as for an OSC without INPs. The preparation process starts with thoroughly cleaning the transparent conducting electrode (TCE)-coated substrate, e.g. ITO-coated glass, via subsequent sonication in distilled (DI) water with detergent, DI water, acetone, and isopropyl alcohol. After that, the substrate is dried in a stream of nitrogen and dried in an oven at elevated temperature to remove any residual solvent. The substrate is then treated with either UV-ozone or oxygen plasma to improve the wettability of the TCE surface and to achieve homogeneous coating of the first charge transport layer. The first CTL can be a HTL or ETL depending on the desired geometry as discussed in section 2. The CTL solution is spin coated on top of the TCE at a specific spinning speed (rpm) to obtain the optimum film thickness (typically up to 50 nm) followed by thermal treatment which depends on the deposited material. Then, the coated substrate should be moved to an inert atmosphere (N<sub>2</sub>-filled glovebox) for the deposition of the active layer. The active blend solution consists of a donor: acceptor mixture dissolved in an appropriate solvent with an optimum concentration and D: A ratio. Spin coating is also utilized to deposit the photoactive layer with the desired thickness. The deposited active layer can be subjected to a thermal or solvent annealing step to improve its morphology. Then, the top CTL can be spin coated or otherwise the substrate is moved to a vacuum deposition chamber to deposit the top CTL and/or the top metal electrode. Finally, the fabricated device should be encapsulated for improved stability [189-191].

The INPs can be incorporated within the charge transport layers, the photoactive layer or at the interfaces between the layers depending on the doping NPs. When the INPs are added to the charge transport layers or to the active blend, the NPs are mixed with the solution of the doped layer to be spin coated after being well dispersed within the solution via stirring and sonication [43, 96]. It should be confirmed that the distribution of the dopant NPs within the doped layer(s) has a crucial impact on the device performance. The aggregation or agglomeration of INPs within the doped layer increases recombination losses and lowers the overall efficiency of the device as discussed in sections 3.1.2., 3.3.1, 5, etc. On the other hand, thermal evaporation was also used to incorporate Cu NPs sandwiched between two thin layers of tungsten trioxide (WO<sub>3</sub>) [88]. In case of magnetic NPs, the dopant NPs can be spin coated under an external magnetic field for the alignment of magnetic dipoles within the active layer, which in turn leads to enhance device performance as discussed in section 3.4.2. For up- and down conversion NPs, other approaches in addition to the spin coating of the doped layer solution

have been reported. These approaches include spray coating of the wavelength-conversion layer at the front of the glass substrate such as that shown in Fig. 23(c). Moreover, the light-converting layer can be pressed and fixed at either the rear or the front side of the device (Fig. 23 (a & b)). The purpose of using the up- or down-conversion layer at the front or back side of the device rather than being doped within the device layers is to avoid disturbing the carrier transport features of the device as discussed in section 3.5.1.1.

# 5. The impact of different types of INPs on the lifetime and cost of OPVs

The lifetime and cost of the device are vital factors for the large-scale production of OPVs. In addition to the PCE-enhancement, the implementation of INPs can also have a positive impact on the stability of OPVs. For instance, DC NPs as well as low cost MNPs (e.g. Al) were found to have a positive impact on device stability. The exposure of OPV to real-world operation conditions of oxygen (air) and moisture commonly leads to photo-oxidation reactions. These reactions result in compositional changes, which eventually lead to a decline of the photovoltaic parameters and hence overall device performance [49, 191-193]. The application of DC NPs for OPVs shows potential to improve the stability of the device as it reduces the amount of UV-radiation reaching the active layer and hence inhibiting degradation reactions of the active blend [4, 188]. Alternatively, Al NPs have shown promise to improve the stability of OPVs when used as dopants to their photoactive layer due to morphology improvements that reduce photo-oxidation of the donor polymer. This photo degradation within the active layer of the device is predominantly induced by singlet oxygen. The energy needed to excite molecular oxygen into singlet oxygen is provided by the triplet excitons of the donor polymer. The presence of metal NPs such as Au and Al within the active blend of the device was found to suppress triplet excitons (through recombination) and hence the formation of singlet oxygen is inhibited and the device stability improved [86, 194].

An additional advantage of using INPs for OPVs is their low cost due to their inexpensive synthesis methods as well as small concentrations. Moreover, these nano-dopants are mixed with the solutions of the doped layers before deposition, thus causing no further expenses during the device fabrication process. In addition, the improvements achieved in performance (either PCE or lifetime) as a result of the addition of different NPs can offset their costs compared to pristine devices. The addition of NPs can have a dual benefit as it may improve both, the efficiency and stability of OPVs. However, it should be noted that improving the efficiency of the device may have a negative impact on its stability. For example, the addition of magnetic NPs to increase the concentration of triplet excitons in the active layer, through intersystem crossing process, can impact the long-term stability of the device under continuous illumination. Triplet excitons, however, can result in photo-oxidation of the donor polymer. Therefore, the selection of the type and concentration of the dopant NPs must be made precisely to maximize their benefits at the lowest cost possible.

# 6. Summary and perspectives

To conclude, the progress in the performance of organic solar cells based on the implementation of different categories of inorganic nanoparticles was reviewed. Different categories of INPs can enhance the performance of OPVs by increasing the light absorption and/or enhancing the dissociation of the photo-generated excitons as well as carrier collection:

The incorporation of metal nano particles (MNPs) into the active layer or/and the buffer layers significantly improved optical absorption due to localized surface Plasmon resonance (LSPR) and light scattering. LSPR strengthens the electromagnetic field close to the surface of MNPs resulting in an enhanced absorption. In addition, scattering increases the path length of the incident photons within

the active layer, which results in higher probability of light interaction with the absorber material. Different metals such as noble metals (e.g. Ag and Au) and low-cost metals such as Al and Cu have been used to produce plasmonic OPVs. To broaden the absorption spectrum of OPVs, both up- and down-converters (UC & DC) based on rare earth metal NPs have been widely investigated. The application of UC NPs aims to convert sub-band gap photons (NIR) into visible light that can be absorbed by the device to enhance the photo-current. Furthermore, DC NPs possess dual functions through the conversion of the above-band gap photons (mainly UV) into visible light, hence increasing the PCE and reducing the amount of UV reaching the core of the device, which, increases the lifetime of the corresponding device.

The low electric permittivity of organic semiconductors leads, upon the absorption of light, to the formation of excitons instead of free charge carriers. In order to contribute to the photocurrent, excitons must be dissociated into free carriers before recombination. An appropriate morphology and nanoscale interpenetrating networks within the active layer should be formed for efficient diffusion of excitons towards the D/A interface, where dissociation takes place. Different nano-dopants such as semiconducting and metal NPs were found to improve the morphology of the active layer and hence device performance. Furthermore, the incorporation of NPs with high electric permittivity into the active layer showed promising potential to improve the dissociation of excitons through reducing the Coulomb attraction between the electron and the hole.

Excitons can exist in either singlet or triplet states, with the lifetime and diffusion length of triplet-state excitons orders of magnitude higher than those of their singlet state counterparts. Thus, increasing the population of triplet excitons reduces recombination losses. The interaction between a weak magnetic field and singlet excitons induces the intersystem crossing effect, resulting in the conversion of singlet into the long-lived triplet excitons. Thus, the incorporation of ferromagnetic NPs such as  $Fe_3O_4$  was proposed as an effective strategy to reduce recombination losses and to enhance device efficiency. Moreover, the application of a magnetostatic field during the deposition of the active layer solution, which contains magnetic NPs, induces a coercive electric field as a result of charge distribution on the surface of the NPs. This electric field greatly improves the sweep-out of excitons and charge transfer through the device, leading to efficient carrier collection at the respective electrodes.

Despite the enhancement in the performance of OPVs achieved with the application of INPs as discussed in this review, further research is this area is still needed. The incorporation of two or more types of NPs simultaneously within the structure of OPVs can combine multiple features, which can consequently lead to a highly improved device efficiency and lifetime. The addition of any type of NPs to OPVs can have a negative impact on the device performance unless it is properly distributed within the doped layer. The aggregation of the dopant NPs disturbs the diffusion of excitons and the transfer of the charge carriers, hence recombination increases as a result. Morphology enhancement and surface modification strategies such as plasma treatment and solvent annealing may help to optimize the configuration of dopant NPs and the morphology of the device. Alkaline-earth metals such as Mg, Be, Sr etc. can be added to charge transport layers to improve charge extraction. New categories of INPs may also contribute to the improvement of OPV performances of in the future.

# **Acknowledgement**

Michael S. A. Kamel would like to acknowledge financial support by James Cook University through a JCUPRS scholarship.

#### **Conflicts of interest**

#### References

- [1] Alkhalayfeh MA, Aziz AA, Pakhuruddin MZ. An overview of enhanced polymer solar cells with embedded plasmonic nanoparticles. Renewable and Sustainable Energy Reviews. 2021;141:110726.
- [2] Liu X, Chen H, Tan S. Overview of high-efficiency organic photovoltaic materials and devices. Renewable and sustainable energy reviews. 2015;52:1527-38.
- [3] Zhao J, Li Y, Yang G, Jiang K, Lin H, Ade H, et al. Efficient organic solar cells processed from hydrocarbon solvents. Nature Energy. 2016;1:15027.
- [4] Grossiord N, Kroon JM, Andriessen R, Blom PW. Degradation mechanisms in organic photovoltaic devices. Organic Electronics. 2012;13:432-56.
- [5] Liu Q, Jiang Y, Jin K, Qin J, Xu J, Li W, et al. 18% Efficiency organic solar cells. Science Bulletin. 2020;65:272-5.
- [6] Li C, Zhou J, Song J, Xu J, Zhang H, Zhang X, et al. Non-fullerene acceptors with branched side chains and improved molecular packing to exceed 18% efficiency in organic solar cells. Nature Energy. 2021;6:605-13.
- [7] Cui Y, Xu Y, Yao H, Bi P, Hong L, Zhang J, et al. Single-Junction Organic Photovoltaic Cell with 19% Efficiency. Advanced Materials. 2021;33:2102420.
- [8] Liang Y, Xu Z, Xia J, Tsai ST, Wu Y, Li G, et al. For the Bright Future—Bulk Heterojunction Polymer Solar Cells with Power Conversion Efficiency of 7.4. Advanced Materials. 2010;22:E135-E8.
- [9] Rafique S, Abdullah SM, Sulaiman K, Iwamoto M. Fundamentals of bulk heterojunction organic solar cells: An overview of stability/degradation issues and strategies for improvement. Renewable and Sustainable Energy Reviews. 2018;84:43-53.
- [10] Riede M, Spoltore D, Leo K. Organic Solar Cells—The Path to Commercial Success. Advanced Energy Materials. 2021;11:2002653.
- [11] Ahmad Z, Najeeb MA, Shakoor R, Al-Muhtaseb SA, Touati F. Limits and possible solutions in quantum dot organic solar cells. Renewable and Sustainable Energy Reviews. 2018;82:1551-64.
- [12] Kumavat PP, Sonar P, Dalal DS. An overview on basics of organic and dye sensitized solar cells, their mechanism and recent improvements. Renewable and Sustainable Energy Reviews. 2017;78:1262-87.
- [13] Zhao J, Li Y, Yang G, Jiang K, Lin H, Ade H, et al. Efficient organic solar cells processed from hydrocarbon solvents. Nature Energy. 2016;1:1-7.
- [14] Zhang Z, Yuan J, Wei Q, Zou Y. Small-Molecule Electron Acceptors for Efficient Non-fullerene Organic Solar Cells. Frontiers in Chemistry. 2018;6.
- [15] Blom PW, Mihailetchi VD, Koster LJA, Markov DE. Device physics of polymer: fullerene bulk heterojunction solar cells. Advanced Materials. 2007;19:1551-66.
- [16] Kirchartz T, Taretto K, Rau U. Efficiency limits of organic bulk heterojunction solar cells. The Journal of Physical Chemistry C. 2009;113:17958-66.
- [17] Bünzli J-CG, Chauvin A-S. Chapter 261 Lanthanides in Solar Energy Conversion. In: Bünzli J-CG, Pecharsky VK, editors. Handbook on the Physics and Chemistry of Rare Earths: Elsevier; 2014. p. 169-281.
- [18] Kesavan AV, Kumar M, Rao AD, Ramamurthy PC. Light management through up-conversion and scattering mechanism of rare earth nanoparticle in polymer photovoltaics. Optical Materials. 2019;94:286-93.
- [19] Yang C, Zhao C, Sun Y, Li Q, Islam MR, Liu K, et al. Optical management in organic photovoltaic devices. Carbon Energy. 2021;3:4-23.
- [20] Nam YM, Huh J, Jo WH. Optimization of thickness and morphology of active layer for high performance of bulk-heterojunction organic solar cells. Solar Energy Materials and Solar Cells. 2010;94:1118-24.

- [21] Ulum M, Sesa E, Belcher W. The effect of active layer thickness on P3HT: PCBM nanoparticulate organic photovoltaic device performance. Journal of Physics: Conference Series: IOP Publishing; 2019. p. 012025.
- [22] Ho CHY, Kothari J, Fu X, So F. Interconnecting layers for tandem organic solar cells. Materials Today Energy. 2021;21:100707.
- [23] Gusain A, Faria RM, Miranda PB. Polymer Solar Cells—Interfacial Processes Related to Performance Issues. Frontiers in Chemistry. 2019;7.
- [24] Colladet K, Nicolas M, Goris L, Lutsen L, Vanderzande D. Low-band gap polymers for photovoltaic applications. Thin Solid Films. 2004;451:7-11.
- [25] Dhanabalan A, Van Duren JKJ, Van Hal PA, Van Dongen JLJ, Janssen RAJ. Synthesis and characterization of a low bandgap conjugated polymer for bulk heterojunction photovoltaic cells. Advanced Funtional Materials. 2001;11:255-62.
- [26] Liang Y, Wu Y, Feng D, Tsai S-T, Son H-J, Li G, et al. Development of New Semiconducting Polymers for High Performance Solar Cells. Journal of the American Chemical Society. 2009;131:56-7.
- [27] Zou Y. Small-Molecule Electron Acceptors for Efficient Non-fullerene Organic Solar Cells. Frontiers in chemistry. 2018;6:414.
- [28] Ma W, Yang C, Gong X, Lee K, Heeger AJ. Thermally Stable, Efficient Polymer Solar Cells with Nanoscale Control of the Interpenetrating Network Morphology. Advanced Functional Materials. 2005;15:1617-22.
- [29] Zhang Y, Li Z, Wakim S, Alem S, Tsang S-W, Lu J, et al. Bulk heterojunction solar cells based on a new low-band-gap polymer: Morphology and performance. Organic Electronics. 2011;12:1211-5.
- [30] Li G, Yao Y, Yang H, Shrotriya V, Yang G, Yang Y. "Solvent annealing" effect in polymer solar cells based on poly (3-hexylthiophene) and methanofullerenes. Advanced Functional Materials. 2007;17:1636-44.
- [31] Molamohammadi S, Nia SA, Jalili YS. Improvement of inverted structure organic solar cells by Ar plasma treatment on P3HT: PC61BM active layer. Sustainable Energy Technologies and Assessments. 2019;34:43-8.
- [32] Gao HL, Zhang XW, Meng JH, Yin ZG, Zhang LQ, Wu JL, et al. Enhanced efficiency in polymer solar cells via hydrogen plasma treatment of ZnO electron transport layers. Journal of Materials Chemistry A. 2015;3:3719-25.
- [33] Papamakarios V, Polydorou E, Soultati A, Droseros N, Tsikritzis D, Douvas AM, et al. Surface modification of ZnO layers via hydrogen plasma treatment for efficient inverted polymer solar cells. ACS applied materials & interfaces. 2016;8:1194-205.
- [34] Lin R, Wright M, Puthen Veettil B, Uddin A. Enhancement of ternary blend organic solar cell efficiency using PTB7 as a sensitizer. Synthetic Metals. 2014;192:113-8.
- [35] Pan M-A, Lau T-K, Tang Y, Wu Y-C, Liu T, Li K, et al. 16.7%-efficiency ternary blended organic photovoltaic cells with PCBM as the acceptor additive to increase the open-circuit voltage and phase purity. Journal of Materials Chemistry A. 2019;7:20713-22.
- [36] Yan T, Song W, Huang J, Peng R, Huang L, Ge Z. 16.67% rigid and 14.06% flexible organic solar cells enabled by ternary heterojunction strategy. Advanced Materials. 2019.
- [37] Zuo X, Xue J, Liming D. Ternary organic solar cells offer 14% power conversion efficiency. 科学通报:英文版. 2017;62:1562-4.
- [38] Zhang S, Ma X, Xu C, Xu W, Jeong SY, Woo HY, et al. Boosted efficiency over 18.1% of polymer solar cells by employing large extinction coefficients material as the third component. Macromolecular Rapid Communications. 2022:2200345.
- [39] Xu C, Ma X, Zhao Z, Jiang M, Hu Z, Gao J, et al. Over 17.6% Efficiency Organic Photovoltaic Devices with Two Compatible Polymer Donors. Solar RRL. 2021;5:2100175.
- [40] Wang X, Sun Q, Gao J, Wang J, Xu C, Ma X, et al. Recent Progress of Organic Photovoltaics with Efficiency over 17%. Energies. 2021;14:4200.

- [41] Xu W, Ma X, Son JH, Jeong SY, Niu L, Xu C, et al. Smart Ternary Strategy in Promoting the Performance of Polymer Solar Cells Based on Bulk-Heterojunction or Layer-By-Layer Structure. Small. 2022;18:2104215.
- [42] Wang DH, Park KH, Seo JH, Seifter J, Jeon JH, Kim JK, et al. Enhanced power conversion efficiency in PCDTBT/PC70BM bulk heterojunction photovoltaic devices with embedded silver nanoparticle clusters. Advanced Energy Materials. 2011;1:766-70.
- [43] Gebhardt RS, Du P, Peer A, Rock M, Kessler MR, Biswas R, et al. Utilizing Wide Band Gap, High Dielectric Constant Nanoparticles as Additives in Organic Solar Cells. The Journal of Physical Chemistry C. 2015;119:23883-9.
- [44] Ohno H. A window on the future of spintronics. Nature materials. 2010;9:952-4.
- [45] Liu Z, Seo S, Lee E-C. Improvement of power conversion efficiencies in Cr2O3-nanoparticle-embedded polymer solar cells. Applied Physics Letters. 2013;103:180 1.
- [46] Oh SH, Heo SJ, Yang JS, Kim HJ. Effects of ZnO nanoparticles on P3HT: PCBM organic solar cells with DMF-modulated PEDOT: PSS buffer layers. ACS applied materials & interfaces. 2013;5:11530-4.
- [47] Salim E, Bobbara S, Oraby A, Nunzi J. Copper oxide nanoparticle doped bulk-heterojunction photovoltaic devices. Synthetic Metals. 2019;252:21-8.
- [48] Scharber MC, Sariciftci NS. Efficiency of bulk-heterojunction organic solar cells. Progress in Polymer Science. 2013;38:1929-40.
- [49] Uddin A, Upama MB, Yi H, Duan L. Encapsulation of organic and perovskite solar cells: a review. Coatings. 2019;9:65.
- [50] Yu G, Gao J, Hummelen JC, Wudl F, Heeger AJ. Polymer photovoltaic cells: enhanced efficiencies via a network of internal donor-acceptor heterojunctions. Science. 1995;270:1789-91.
- [51] Smets AH, Jäger K, Isabella O, van Swaaij R, Zeman M. Solar Energy: The physics and engineering of photovoltaic conversion technologies and systems: UIT; 2016.
- [52] Xu W, Li X, Jeong SY, Son JH, Zhou Z, Jiang Q, et al. Achieving 17.5% efficiency for polymer solar cells via a donor and acceptor layered optimization strategy. Journal of Materials Chemistry C. 2022;10:5489-96.
- [53] Gusain A, Faria RM, Miranda PB. Polymer Solar Cells—Interfacial Processes Related to Performance Issues. Frontiers in chemistry. 2019;7.
- [54] Wright M, Uddin A. Organic—inorganic hybrid solar cells: A comparative review. Solar energy materials and solar cells. 2012;107:87-111.
- [55] Tamai Y, Ohkita H, Benten H, Ito S. Exciton Diffusion in Conjugated Polymers: From Fundamental Understanding to Improvement in Photovoltaic Conversion Efficiency. The Journal of Physical Chemistry Letters. 2015;6:3417-28.
- [56] Mihailetchi V, Koster L, Hummelen J, Blom P. Photocurrent generation in polymer-fullerene bulk heterojunctions. Physical review letters. 2004;93:216601.
- [57] Shuttle CG, O'Regan B, Ballantyne AM, Nelson J, Bradley DD, Durrant JR. Bimolecular recombination losses in polythiophene: Fullerene solar cells. Physical Review B. 2008;78:113201.
- [58] Shoaee S, Stolterfoht M, Neher D. The Role of Mobility on Charge Generation, Recombination, and Extraction in Polymer-Based Solar Cells. Advanced Energy Materials. 2018;8:1703355.
- [59] Masson J-F. Portable and field-deployed surface plasmon resonance and plasmonic sensors. Analyst. 2020;145:3776-800.
- [60] Kelly KL, Coronado E, Zhao LL, Schatz GC. The Optical Properties of Metal Nanoparticles: The Influence of Size, Shape, and Dielectric Environment. The Journal of Physical Chemistry B. 2003;107:668-77.
- [61] Sha WE, Choy WC, Liu YG, Cho Chew W. Near-field multiple scattering effects of plasmonic nanospheres embedded into thin-film organic solar cells. Applied Physics Letters. 2011;99:199.
- [62] Uddin A, Yang X. Surface plasmonic effects on organic solar cells. Journal of nanoscience and nanotechnology. 2014;14:1099-119.
- [63] Baek S-W, Noh J, Lee C-H, Kim B, Seo M-K, Lee J-Y. Plasmonic Forward Scattering Effect in Organic Solar Cells: A Powerful Optical Engineering Method. Scientific Reports. 2013;3:1726.

- [64] Wu B, Wu X, Guan C, Fai Tai K, Yeow EKL, Jin Fan H, et al. Uncovering loss mechanisms in silver nanoparticle-blended plasmonic organic solar cells. Nature Communications. 2013;4:2004.
- [65] Feng L, Niu M, Wen Z, Hao X. Recent advances of plasmonic organic solar cells: Photophysical investigations. Polymers. 2018;10:123.
- [66] Gan Q, Bartoli FJ, Kafafi ZH. Plasmonic-Enhanced Organic Photovoltaics: Breaking the 10% Efficiency Barrier. Advanced Materials. 2013;25:2385-96.
- [67] Kim K, Carroll DL. Roles of Au and Ag nanoparticles in efficiency enhancement of poly(3-octylthiophene)/C60 bulk heterojunction photovoltaic devices. Applied Physics Letters. 2005;87:203113.
- [68] Wang DH, Kim DY, Choi KW, Seo JH, Im SH, Park JH, et al. Enhancement of donor—acceptor polymer bulk heterojunction solar cell power conversion efficiencies by addition of Au nanoparticles. Angewandte Chemie International Edition. 2011;50:5519-23.
- [69] Paci B, Spyropoulos GD, Generosi A, Bailo D, Albertini VR, Stratakis E, et al. Enhanced structural stability and performance durability of bulk heterojunction photovoltaic devices incorporating metallic nanoparticles. Advanced Functional Materials. 2011;21:3573-82.
- [70] Wu J-L, Chen F-C, Hsiao Y-S, Chien F-C, Chen P, Kuo C-H, et al. Surface plasmonic effects of metallic nanoparticles on the performance of polymer bulk heterojunction solar cells. ACS nano. 2011;5:959-67.
- [71] Spyropoulos G, Stylianakis M, Stratakis E, Kymakis E. Plasmonic organic photovoltaics doped with metal nanoparticles. Photonics and Nanostructures-Fundamentals and Applications. 2011;9:184-9.
- [72] Yang X, Chueh CC, Li CZ, Yip HL, Yin P, Chen H, et al. High-Efficiency Polymer Solar Cells Achieved by Doping Plasmonic Metallic Nanoparticles into Dual Charge Selecting Interfacial Layers to Enhance Light Trapping. Advanced Energy Materials. 2013;3:666-73.
- [73] Xie FX, Choy WC, Wang CC, Sha WE, Fung DD. Improving the efficiency of polymer solar cells by incorporating gold nanoparticles into all polymer layers. Applied Physics Letters. 2011;99:219.
- [74] Li X, Choy WC, Huo L, Xie F, Sha WE, Ding B, et al. Dual plasmonic nanostructures for high performance inverted organic solar cells. Advanced Materials. 2012;24:3046-52.
- [75] Lu L, Luo Z, Xu T, Yu L. Cooperative plasmonic effect of Ag and Au nanoparticles on enhancing performance of polymer solar cells. Nano letters. 2012;13:59-64.
- [76] Singh A, Dey A, Iyer PK. Collective effect of hybrid Au-Ag nanoparticles and organic-inorganic cathode interfacial layers for high performance polymer solar cell. Solar Energy. 2018;173:429-36.
- [77] Kaçuş H, Aydoğan Ş, Biber M, Metin Ö, Sevim M. The power conversion efficiency optimization of the solar cells by doping of (Au: Ag) nanoparticles into P3HT: PCBM active layer prepared with chlorobenzene and chloroform solvents. Materials Research Express. 2019;6:095104.
- [78] Baek S-W, Noh J, Lee C-H, Kim B, Seo M-K, Lee J-Y. Plasmonic forward scattering effect in organic solar cells: a powerful optical engineering method. Scientific reports. 2013;3:1726.
- [79] Liu X-H, Hou L-X, Wang J-F, Liu B, Yu Z-S, Ma L-Q, et al. Plasmonic-enhanced polymer solar cells with high efficiency by addition of silver nanoparticles of different sizes in different layers. Solar Energy. 2014;110:627-35.
- [80] Li X, Choy WCH, Lu H, Sha WE, Ho AHP. Efficiency enhancement of organic solar cells by using shape-dependent broadband plasmonic absorption in metallic nanoparticles. Advanced Functional Materials. 2013;23:2728-35.
- [81] Yao K, Salvador M, Chueh CC, Xin XK, Xu YX, Dequilettes DW, et al. A general route to enhance polymer solar cell performance using plasmonic nanoprisms. Advanced Energy Materials. 2014;4:1400206.
- [82] Ng A, Yiu WK, Foo Y, Shen Q, Bejaoui A, Zhao Y, et al. Enhanced performance of PTB7: PC71BM solar cells via different morphologies of gold nanoparticles. ACS applied materials & interfaces. 2014;6:20676-84.
- [83] Li Q, Wang F, Bai Y, Xu L, Yang Y, Yan L, et al. Decahedral-shaped Au nanoparticles as plasmonic centers for high performance polymer solar cells. Organic Electronics. 2017;43:33-40.

- [84] He Y, Liu C, Li J, Zhang X, Li Z, Shen L, et al. Improved power conversion efficiency of inverted organic solar cells by incorporating Au nanorods into active layer. ACS applied materials & interfaces. 2015;7:15848-54.
- [85] Szeremeta J, Nyk M, Chyla A, Strek W, Samoc M. Enhancement of photoconduction in a conjugated polymer through doping with copper nanoparticles. Optical Materials. 2011;33:1372-6.
- [86] Kakavelakis G, Stratakis E, Kymakis E. Aluminum nanoparticles for efficient and stable organic photovoltaics. Rsc Advances. 2013;3:16288-91.
- [87] Sygletou M, Kakavelakis G, Paci B, Generosi A, Kymakis E, Stratakis E. Enhanced stability of aluminum nanoparticle-doped organic solar cells. ACS applied materials & interfaces. 2015;7:17756-64
- [88] Shen P, Liu Y, Long Y, Shen L, Kang B. High-performance polymer solar cells enabled by copper nanoparticles-induced plasmon resonance enhancement. The Journal of Physical Chemistry C. 2016;120:8900-6.
- [89] Tang M, Sun B, Zhou D, Gu Z, Chen K, Guo J, et al. Broad-band plasmonic Cu-Au bimetallic nanoparticles for organic bulk heterojunction solar cells. Organic Electronics. 2016;38:213-21.
- [90] Oseni SO, Mola GT. Effects of metal-decorated nanocomposite on inverted thin film organic solar cell. Journal of Physics and Chemistry of Solids. 2019;130:120-6.
- [91] Huang S, Tang Y, Dang Y, Xu X, Dong Q, Kang B, et al. Low-temperature solution-processed Mg: SnO2 nanoparticles as an effective cathode interfacial layer for inverted polymer solar cell. ACS Sustainable Chemistry & Engineering. 2018;6:6702-10.
- [92] Lenes M, Kooistra F, Hummelen JC, Van Severen I, Lutsen L, Vanderzande D, et al. Charge dissociation in polymer: fullerene bulk heterojunction solar cells with enhanced permittivity. Journal of Applied Physics. 2008;104:114517.
- [93] Onsager L. Initial Recombination of Ions. Physical Review. 1938;54:554-7.
- [94] Langevin P. L'ionization des gaz. Ann Chim Phys. 1903;28:289-384.
- [95] Elumalai NK, Uddin A. Open circuit voltage of organic solar cells: an in-depth review. Energy & Environmental Science. 2016;9:391-410.
- [96] Black D, Salaoru I, Paul S. Route to enhance the efficiency of organic photovoltaic solar cells-by adding ferroelectric nanoparticles to P3HT/PCBM admixture. EPJ Photovoltaics. 2014;5:50403.
- [97] Shao P, Chen X, Guo X, Zhang W, Chang F, Liu Q, et al. Facile embedding of SiO2 nanoparticles in organic solar cells for performance improvement. Organic Electronics. 2017;50:77-81.
- [98] Celik D, Krueger M, Veit C, Schleiermacher HF, Zimmermann B, Allard S, et al. Performance enhancement of CdSe nanorod-polymer based hybrid solar cells utilizing a novel combination of post-synthetic nanoparticle surface treatments. Solar Energy Materials and Solar Cells. 2012;98:433-40.
- [99] Ren S, Chang L-Y, Lim S-K, Zhao J, Smith M, Zhao N, et al. Inorganic—organic hybrid solar cell: bridging quantum dots to conjugated polymer nanowires. Nano letters. 2011;11:3998-4002.
- [100] Zhou Y, Eck M, Veit C, Zimmermann B, Rauscher F, Niyamakom P, et al. Efficiency enhancement for bulk-heterojunction hybrid solar cells based on acid treated CdSe quantum dots and low bandgap polymer PCPDTBT. Solar Energy Materials and Solar Cells. 2011;95:1232-7.
- [101] Alivisatos AP. Semiconductor clusters, nanocrystals, and quantum dots. science. 1996;271:933-7.
- [102] Liu CY, Holman ZC, Kortshagen UR. Optimization of Si NC/P3HT hybrid solar cells. Advanced Functional Materials. 2010;20:2157-64.
- [103] Borchert H. Elementary processes and limiting factors in hybrid polymer/nanoparticle solar cells. Energy & Environmental Science. 2010;3:1682-94.
- [104] Yu Y-Y, Chien W-C, Ko Y-H, Chan Y-C, Liao S-C. Enhancement of photovoltaic performance in P3HT hybrid solar cell by blending colloidal TiO2 nanocrystal. Current Applied Physics. 2012;12:S7-S13.
- [105] Park SH, Roy A, Beaupré S, Cho S, Coates N, Moon JS, et al. Bulk heterojunction solar cells with internal quantum efficiency approaching 100%. Nature photonics. 2009;3:297.

- [106] Zhu T, Zhang Y, Li Y, Song X, Liu Z, Wen S, et al. Acceptor-rich bulk heterojunction polymer solar cells with balanced charge mobilities. Organic Electronics. 2017;51:16-24.
- [107] Lee C-T, Lee C-H. Conversion efficiency improvement mechanisms of polymer solar cells by balance electron—hole mobility using blended P3HT:PCBM:pentacene active layer. Organic Electronics. 2013;14:2046-50.
- [108] Hamed MS, Oseni SO, Kumar A, Sharma G, Mola GT. Nickel sulphide nano-composite assisted hole transport in thin film polymer solar cells. Solar Energy. 2020;195:310-7.
- [109] Liao H-C, Tsao C-S, Lin T-H, Jao M-H, Chuang C-M, Chang S-Y, et al. Nanoparticle-Tuned Self-Organization of a Bulk Heterojunction Hybrid Solar Cell with Enhanced Performance. ACS Nano. 2012;6:1657-66.
- [110] Khan MT, Bhargav R, Kaur A, Dhawan SK, Chand S. Effect of cadmium sulphide quantum dot processing and post thermal annealing on P3HT/PCBM photovoltaic device. Thin Solid Films. 2010;519:1007-11.
- [111] Taukeer Khan M, Kaur A, Dhawan S, Chand S. In-Situ growth of cadmium telluride nanocrystals in poly (3-hexylthiophene) matrix for photovoltaic application. Journal of Applied Physics. 2011;110:044509.
- [112] Itskos G, Othonos A, Rauch T, Tedde SF, Hayden O, Kovalenko MV, et al. Optical Properties of Organic Semiconductor Blends with Near-Infrared Quantum-Dot Sensitizers for Light Harvesting Applications. Advanced Energy Materials. 2011;1:802-12.
- [113] Lu Y, Hou Y, Wang Y, Feng Z, Liu X, Lü Y. Effect of monodisperse Cu2S nanodisks on photovoltaic performance of P3HT/PCBM polymer solar cells. Synthetic Metals. 2011;161:906-10.
- [114] Sharma R, Bhalerao S, Gupta D. Effect of incorporation of CdS NPs on performance of PTB7: PCBM organic solar cells. Organic Electronics. 2016;33:274-80.
- [115] Zheng Z, Zhang S, Wang J, Zhang J, Zhang D, Zhang Y, et al. Exquisite modulation of ZnO nanoparticle electron transporting layer for high-performance fullerene-free organic solar cell with inverted structure. Journal of Materials Chemistry A. 2019;7:3570-6.
- [116] Upama MB, Elumalai NK, Mahmud MA, Xu C, Wang D, Wright M, et al. Enhanced electron transport enables over 12% efficiency by interface engineering of non-fullerene organic solar cells. Solar Energy Materials and Solar Cells. 2018;187:273-82.
- [117] Sajjad MT, Ruseckas A, Samuel IDW. Enhancing Exciton Diffusion Length Provides New Opportunities for Organic Photovoltaics. Matter. 2020;3:341-54.
- [118] González DM, Körstgens V, Yao Y, Song L, Santoro G, Roth SV, et al. Improved Power Conversion Efficiency of P3HT: PCBM Organic Solar Cells by Strong Spin—Orbit Coupling-Induced Delayed Fluorescence. Advanced Energy Materials. 2015;5:1401770.
- [119] Luppi BT, Majak D, Gupta M, Rivard E, Shankar K. Triplet excitons: improving exciton diffusion length for enhanced organic photovoltaics. Journal of Materials Chemistry A. 2019;7:2445-63.
- [120] Kim Y, Bradley DD. Bright red emission from single layer polymer light-emitting devices based on blends of regioregular P3HT and F8BT. Current Applied Physics. 2005;5:222-6.
- [121] Shuttle C, Hamilton R, O'Regan B, Nelson Ja, Durrant J. Charge-density-based analysis of the current–voltage response of polythiophene/fullerene photovoltaic devices. Proceedings of the National Academy of Sciences. 2010;107:16448-52.
- [122] Xu B, Holdcroft S. Phosphorescence and delayed fluorescence of poly (3-hexylthiophene) films. Thin Solid Films. 1994;242:174-7.
- [123] Guo F, Kim Y-G, Reynolds JR, Schanze KS. Platinum—acetylide polymer based solar cells: involvement of the triplet state for energy conversion. Chemical communications. 2006:1887-9.
- [124] Köhler A, Wittmann H, Friend RH, Khan MS, Lewis J. Enhanced photocurrent response in photocells made with platinum-poly-yne/C60 blends by photoinduced electron transfer. Synthetic metals. 1996;77:147-50.
- [125] Xu Z, Hu B, Howe J. Improvement of photovoltaic response based on enhancement of spin-orbital coupling and triplet states in organic solar cells. Journal of Applied Physics. 2008;103:043909.

- [126] Shakya P, Desai P, Kreouzis T, Gillin W, Tuladhar S, Ballantyne A, et al. The effect of applied magnetic field on photocurrent generation in poly-3-hexylthiophene:[6, 6]-phenyl C61-butyric acid methyl ester photovoltaic devices. Journal of Physics: Condensed Matter. 2008;20:452203.
- [127] Desai P, Shakya P, Kreouzis T, Gillin W. Magnetoresistance in organic light-emitting diode structures under illumination. Physical Review B. 2007;76:235202.
- [128] Zhang W, Xu Y, Wang H, Xu C, Yang S. Fe3O4 nanoparticles induced magnetic field effect on efficiency enhancement of P3HT: PCBM bulk heterojunction polymer solar cells. Solar Energy Materials and Solar Cells. 2011;95:2880-5.
- [129] Pereira M, Lima F, Ribeiro T, da Silva M, Almeida R, Barros E, et al. Application of Fe-doped SnO2 nanoparticles in organic solar cells with enhanced stability. Optical Materials. 2017;64:548-56.
- [130] González DM, Körstgens V, Yao Y, Song L, Santoro G, Roth SV, et al. Improved Power Conversion Efficiency of P3HT:PCBM Organic Solar Cells by Strong Spin—Orbit Coupling-Induced Delayed Fluorescence. Advanced Energy Materials. 2015;5:1401770.
- [131] Kovalenko A, Yadav RS, Pospisil J, Zmeskal O, Karashanova D, Heinrichová P, et al. Towards improved efficiency of bulk-heterojunction solar cells using various spinel ferrite magnetic nanoparticles. Organic Electronics. 2016;39:118-26.
- [132] Cowan SR, Banerji N, Leong WL, Heeger AJ. Charge formation, recombination, and sweep-out dynamics in organic solar cells. Advanced Functional Materials. 2012;22:1116-28.
- [133] Hwang JG, Zahn M, O'Sullivan FM, Pettersson LAA, Hjortstam O, Liu R. Effects of nanoparticle charging on streamer development in transformer oil-based nanofluids. Journal of Applied Physics. 2010;107:014310.
- [134] Mørup S, Hansen MF, Frandsen C. Magnetic interactions between nanoparticles. Beilstein journal of nanotechnology. 2010;1:182-90.
- [135] Shvydka D, Karpov V. Nanodipole photovoltaics. Applied Physics Letters. 2008;92:053507.
- [136] Yang T-I, Brown RN, Kempel LC, Kofinas P. Magneto-dielectric properties of polymer–Fe3O4 nanocomposites. Journal of Magnetism and Magnetic Materials. 2008;320:2714-20.
- [137] Wang K, Yi C, Liu C, Hu X, Chuang S, Gong X. Effects of magnetic nanoparticles and external magnetostatic field on the bulk heterojunction polymer solar cells. Scientific reports. 2015;5:1-9.
- [138] Ekins-Daukes N. Routes to high efficiency photovoltaic power conversion. 2013 IEEE 39th Photovoltaic Specialists Conference (PVSC): IEEE; 2013. p. 0013-6.
- [139] Shang Y, Hao S, Yang C, Chen G. Enhancing solar cell efficiency using photon upconversion materials. Nanomaterials. 2015;5:1782-809.
- [140] Bunzli J-CG. Lanthanide luminescence for biomedical analyses and imaging. Chemical reviews. 2010;110:2729-55.
- [141] Bünzli J-CG. Benefiting from the unique properties of lanthanide ions. Accounts of chemical research. 2006;39:53-61.
- [142] Carlos LD, Ferreira RA, de Zea Bermudez V, Julian-Lopez B, Escribano P. Progress on lanthanide-based organic—inorganic hybrid phosphors. Chemical Society Reviews. 2011;40:536-49.
- [143] Lingeshwar Reddy K, Balaji R, Kumar A, Krishnan V. Lanthanide doped near infrared active upconversion nanophosphors: Fundamental concepts, synthesis strategies, and technological applications. Small. 2018;14:1801304.
- [144] Chen G, Ohulchanskyy TY, Kumar R, Ågren H, Prasad PN. Ultrasmall monodisperse NaYF4: Yb3+/Tm3+ nanocrystals with enhanced near-infrared to near-infrared upconversion photoluminescence. ACS nano. 2010;4:3163-8.
- [145] Sun Y, Chen Y, Tian L, Yu Y, Kong X, Zhao J, et al. Controlled synthesis and morphology dependent upconversion luminescence of NaYF4: Yb, Er nanocrystals. Nanotechnology. 2007;18:275609.
- [146] Wang L, Li Y. Na (Y1. 5Na0. 5) F6 single-crystal nanorods as multicolor luminescent materials. Nano Letters. 2006;6:1645-9.

- [147] Chen G, Ohulchanskyy TY, Kachynski A, Ågren H, Prasad PN. Intense visible and near-infrared upconversion photoluminescence in colloidal LiYF4: Er3+ nanocrystals under excitation at 1490 nm. ACS nano. 2011;5:4981-6.
- [148] Chen D, Lei L, Yang A, Wang Z, Wang Y. Ultra-broadband near-infrared excitable upconversion core/shell nanocrystals. Chemical Communications. 2012;48:5898-900.
- [149] Joubert M-F. Photon avalanche upconversion in rare earth laser materials. Optical materials. 1999;11:181-203.
- [150] Ong LC, Gnanasammandhan MK, Nagarajan S, Zhang Y. Upconversion: road to El Dorado of the fluorescence world. Luminescence. 2010;25:290-3.
- [151] Thirumalai J. Luminescence: An Outlook on the Phenomena and their Applications: BoD–Books on Demand; 2016.
- [152] Wang F, Liu X. Recent advances in the chemistry of lanthanide-doped upconversion nanocrystals. Chemical Society Reviews. 2009;38:976-89.
- [153] Kamimura M, Miyamoto D, Saito Y, Soga K, Nagasaki Y. Design of poly (ethylene glycol)/streptavidin coimmobilized upconversion nanophosphors and their application to fluorescence biolabeling. Langmuir. 2008;24:8864-70.
- [154] Singh S, Singh A, Kumar D, Prakash O, Rai S. Efficient UV–visible up-conversion emission in Er 3+/Yb 3+ co-doped La 2 O 3 nano-crystalline phosphor. Applied Physics B. 2010;98:173-9.
- [155] Sudheendra L, Ortalan V, Dey S, Browning ND, Kennedy IM. Plasmonic enhanced emissions from cubic NaYF4: Yb: Er/Tm nanophosphors. Chemistry of Materials. 2011;23:2987-93.
- [156] Sun L-D, Dong H, Zhang P-Z, Yan C-H. Upconversion of rare earth nanomaterials. Annual review of physical chemistry. 2015;66:619-42.
- [157] Boyer J-C, Cuccia LA, Capobianco JA. Synthesis of colloidal upconverting NaYF4: Er3+/Yb3+ and Tm3+/Yb3+ monodisperse nanocrystals. Nano letters. 2007;7:847-52.
- [158] Heer S, Kömpe K, Güdel HU, Haase M. Highly efficient multicolour upconversion emission in transparent colloids of lanthanide-doped NaYF4 nanocrystals. Advanced Materials. 2004;16:2102-5.
- [159] Yi G-S, Chow G-M. Water-soluble NaYF4: Yb, Er (Tm)/NaYF4/polymer core/shell/shell nanoparticles with significant enhancement of upconversion fluorescence. Chemistry of Materials. 2007;19:341-3.
- [160] Mai H-X, Zhang Y-W, Si R, Yan Z-G, Sun L-d, You L-P, et al. High-quality sodium rare-earth fluoride nanocrystals: controlled synthesis and optical properties. Journal of the American Chemical Society. 2006;128:6426-36.
- [161] Thoma R, Insley H, Hebert G. The sodium fluoride-lanthanide trifluoride systems. Inorganic chemistry. 1966;5:1222-9.
- [162] Ding M, Chen D, Yin S, Ji Z, Zhong J, Ni Y, et al. Simultaneous morphology manipulation and upconversion luminescence enhancement of  $\beta$ -NaYF 4: Yb 3+/Er 3+ microcrystals by simply tuning the KF dosage. Scientific reports. 2015;5:12745.
- [163] Soukka T, Rantanen T, Kuningas K. Photon upconversion in homogeneous fluorescence-based bioanalytical assays. Annals of the New York Academy of Sciences. 2008;1130:188-200.
- [164] Sun T, Wang F. Lanthanide-Doped Core—Shell Upconversion Nanophosphors. Phosphors, Up Conversion Nano Particles, Quantum Dots and Their Applications: Springer; 2016. p. 289-309.
- [165] Wang HQ, Batentschuk M, Osvet A, Pinna L, Brabec CJ. Rare-earth ion doped up-conversion materials for photovoltaic applications. Advanced Materials. 2011;23:2675-80.
- [166] Wang H-Q, Stubhan T, Osvet A, Litzov I, Brabec CJ. Up-conversion semiconducting MoO3: Yb/Er nanocomposites as buffer layer in organic solar cells. Solar energy materials and solar cells. 2012;105:196-201.
- [167] Liu C, Chen H, Zhao D, Shen L, He Y, Guo W, et al. The action mechanism of TiO2: NaYF4: Yb3+, Tm3+ cathode buffer layer in highly efficient inverted organic solar cells. Applied Physics Letters. 2014;105:115\_1.

- [168] Chen S, Peng B, Lu F, Mei Y, Cheng F, Deng L, et al. Scattering or Photoluminescence? Major Mechanism Exploration on Performance Enhancement in P3HT-Based Polymer Solar Cells with NaYF4: 2% Er3+, 18% Yb3+ Upconverting Nanocrystals. Advanced Optical Materials. 2014;2:442-9. [169] Zhang X, Zheng K, Liu C, Li H, Li Z, Li J, et al. Enhancing the light-harvesting and charge transport properties of polymer solar cells by embedding NaLuF 4: Yb, Tm nanorods. RSC Advances. 2015;5:32891-6.
- [170] Guo W, Jiang H, Liu C, He Y, Zhang X. The role of NaYF 4 nanoparticles in inverted polymer solar cells. SPIE2014. p. 923328.
- [171] Adikaari AD, Etchart I, Guéring P-H, Bérard M, Silva SRP, Cheetham AK, et al. Near infrared upconversion in organic photovoltaic devices using an efficient Yb3+: Ho3+ Co-doped Ln2BaZnO5 (Ln=Y, Gd) phosphor. Journal of Applied Physics. 2012;111:094502.
- [172] Wu J-L, Chen F-C, Chang S-H, Tan K-S, Tuan H-Y. Upconversion effects on the performance of near-infrared laser-driven polymer photovoltaic devices. Organic Electronics. 2012;13:2104-8.
- [173] Wu J-L, Chen F-C, Chuang M-K, Tan K-S. Near-infrared laser-driven polymer photovoltaic devices and their biomedical applications. Energy & Environmental Science. 2011;4:3374-8.
- [174] De La Mora M, Amelines-Sarria O, Monroy B, Hernández-Pérez C, Lugo J. Materials for downconversion in solar cells: Perspectives and challenges. Solar Energy Materials and Solar Cells. 2017;165:59-71.
- [175] Zhang QY, Huang XY. Recent progress in quantum cutting phosphors. Progress in Materials Science. 2010;55:353-427.
- [176] Zhou X, Shen J, Wang Y, Feng Z, Wang R, Li L, et al. An Efficient Dual-Mode Solar Spectral Modification for c-Si Solar Cells in Tm3+/Yb3+ Codoped Tellurite Glasses. Journal of the American Ceramic Society. 2016;99:2300-5.
- [177] Lim MJ, Ko YN, Chan Kang Y, Jung KY. Enhancement of light-harvesting efficiency of dye-sensitized solar cells via forming TiO2 composite double layers with down/up converting phosphor dispersion. RSC Advances. 2014;4:10039-42.
- [178] Yao N, Huang J, Fu K, Deng X, Ding M, Xu X. Rare earth ion doped phosphors for dye-sensitized solar cells applications. RSC Advances. 2016;6:17546-59.
- [179] Zhu G, Wang X, Li H, Pan L, Sun H, Liu X, et al. Y3Al5O12:Ce phosphors as a scattering layer for high-efficiency dye sensitized solar cells. Chemical Communications. 2012;48:958-60.
- [180] Svrcek V, Yamanari T, Mariotti D, Mitra S, Velusamy T, Matsubara K. A silicon nanocrystal/polymer nanocomposite as a down-conversion layer in organic and hybrid solar cells. Nanoscale. 2015;7:11566-74.
- [181] Wu N, Luo Q, Qiao X, Ma C-Q. The preparation of a Eu3+-doped ZnO bi-functional layer and its application in organic photovoltaics. Materials Research Express. 2015;2:125901.
- [182] Tsai M-L, Wei W-R, Tang L, Chang H-C, Tai S-H, Yang P-K, et al. Si Hybrid Solar Cells with 13% Efficiency via Concurrent Improvement in Optical and Electrical Properties by Employing Graphene Quantum Dots. ACS Nano. 2016;10:815-21.
- [183] Cheng C, Yang J. Hydrothermal Synthesis of \$\hbox{Eu}^{3+}\$ -Doped
- \$\hbox{Y}(\hbox{OH})\_{3}\$ Nanotubes as Downconversion Materials for Efficiency Enhancement of Screen-Printed Monocrystalline Silicon Solar Cells. IEEE Electron Device Letters. 2012;33:697-9.
- [184] Huang C-Y, Wang D-Y, Wang C-H, Chen Y-T, Wang Y-T, Jiang Y-T, et al. Efficient Light Harvesting by Photon Downconversion and Light Trapping in Hybrid ZnS Nanoparticles/Si Nanotips Solar Cells. ACS Nano. 2010;4:5849-54.
- [185] Wang T, Zhang J, Ma W, Luo Y, Wang L, Hu Z, et al. Luminescent solar concentrator employing rare earth complex with zero self-absorption loss. Solar Energy. 2011;85:2571-9.
- [186] Binnemans K. Lanthanide-based luminescent hybrid materials. Chemical reviews. 2009;109:4283-374.
- [187] Huang X, Han S, Huang W, Liu X. Enhancing solar cell efficiency: the search for luminescent materials as spectral converters. Chemical Society Reviews. 2013;42:173-201.

[188] Bu F, Shen W, Zhang X, Wang Y, Belfiore LA, Tang J. Hybrid ZnO electron transport layer by down conversion complexes for dual improvements of photovoltaic and stable performances in polymer solar cells. Nanomaterials. 2020;10:80.

[189] Upama MB, Elumalai NK, Mahmud MA, Wright M, Wang D, Xu C, et al. Interfacial engineering of electron transport layer using Caesium Iodide for efficient and stable organic solar cells. Applied Surface Science. 2017;416:834-44.

[190] Lin R, Wright M, Uddin A. Effects of solvent additive on inverted structure PCPDTBT: PC 71 BM bulk heterojunction organic solar cells. physica status solidi (a). 2013;210:1785-90.

[191] Kamel MS, Oelgemöller M, Jacob MV. Sustainable plasma polymer encapsulation materials for organic solar cells. Journal of Materials Chemistry A. 2022;10:4683-94.

[192] Kawano K, Pacios R, Poplavskyy D, Nelson J, Bradley DDC, Durrant JR. Degradation of organic solar cells due to air exposure. Solar Energy Materials and Solar Cells. 2006;90:3520-30.

[193] Neugebauer H, Brabec C, Hummelen JC, Sariciftci NS. Stability and photodegradation mechanisms of conjugated polymer/fullerene plastic solar cells. Solar Energy Materials and Solar Cells. 2000;61:35-42.

[194] Paci B, Generosi A, Albertini VR, Spyropoulos GD, Stratakis E, Kymakis E. Enhancement of photo/thermal stability of organic bulk heterojunction photovoltaic devices via gold nanoparticles doping of the active layer. Nanoscale. 2012;4:7452-9.